2-8-2011

TREE ROOT ENCROACHMENT ON LEVEE DRAINAGE SYSTEM

Tomomi Ito

Tomomi Ito
Candidate

Civil Engineering
Department

This thesis is approved, and it is acceptable in quality and form for publication:

Approved by the Thesis Committee:

_____, Chairperson

_____

_____

_____

_____

_____

_____

_____

TREE ROOT ENCROACHMENT ON LEVEE DRAINAGE SYSTEM

BY

Tomomi Ito

B.S., Tottori University, Japan, 2008

THESIS

Submitted in Partial Fulfillment of the
Requirements for the Degree of

Master of Science in Civil Engineering

The University of New Mexico
Albuquerque, New Mexico

July, 2010

TREE ROOT ENCROACHMENT ON LEVEE DRAINAGE SYSTEM

BY

Tomomi Ito

ABSTRACT OF THESIS

Submitted in Partial Fulfillment of the
Requirements for the Degree of

Master of Science in Civil Engineering

The University of New Mexico
Albuquerque, New Mexico

July, 2010

TREE ROOT ENCROACHMENT ON LEVEE DRAINAGE SYSTEM

by

Tomomi Ito

M.S., Agricultural Engineering, 2008

ABSTRACT

The objectives of this study were to estimate the influence of roots on the drainage facilities associated with the levees along the middle Rio Grande (MRG), and to suggest an appropriate drainage design. This study consists of three research elements: (1) GIS-based analysis in estimating root distribution along levees, (2) a bench-top experiment, and (3) evaluating a drainage designs using a numerical model.

First, tree crown sizes were measured on GIS-based aerial photography to estimate root distributions. The results were compared with vegetation maps that were created based on field observations. The GIS-based measurements and field measurements showed similar values if the site was covered with a simple vegetation community. Simple canopy shapes improved the precision of the measurements. However, the GIS-based measurement was not accurate for a site with complex vegetation coverage.

The bench-top experiment was conducted to evaluate the effectiveness of two types of geosynthetics as root barriers. A geotextile and a geocomposite were tested in

clear columns filled with soil and/or gravel to simulate six different drainage designs. Two New Mexican plants, Rio Grande cottonwood (*Populus deltoides ssp. wislizeni*) and coyote willow (*Salix exigua*), were selected, and planted in columns. The results showed roots of both species could penetrate through the geotextile and geocomposite. Also, root growth was not affected by the types of root barriers nor drainage material.

For the last study element, HYDRUS-2D was applied to understand the soil water movement in the levee. The typical toe drain and the geocomposite edge drain were considered, and the models were run under the ambient condition (unsaturated) and the flood condition (saturated). As a result, the functions of both drainage designs were close to identical under the ambient condition since it did not result in drainage. In contrast, under the flood condition, the geocomposite edge drain could remove excess water more efficiently than the conventional toe drain.

TABLE OF CONTENTS

LIST OF FIGURES

LIST OF TABLES

CHAPTER 1: INTRODUCTION

1.1 Background of the study

This research concerns the investigation of vegetative barriers for levees. The preliminary research was conducted by The University of New Mexico with support of the United States Army Corps of Engineers (USACE).

The Southwestern United States has a semi-arid climate, and the low precipitation and high evapotranpiration result in sparse vegetation. In Bernalillo County, New Mexico, the middle Rio Grande (MRG) riparian corridor, commonly referred to as Bosque, plays an important role in maintaining ecological diversity and richness in the region.

Many organizations, affiliated national, federal, state, and tribal organizations, are currently involved in ecosystem restoration (U.S. Forest Service Rocky Mountain Research Station, 2008). Current ecosystem management efforts include planting trees to enhance biological and recreational values of Bosque. However, riparian tree roots can degrade flood-control levees, resulting in their failure to perform as designed.

Levees are earthen embankments constructed along rivers to contain floods and are usually subject to hydraulic loading for durations of less than a few weeks annually. Levees are common in many parts of the world (Shields and Gray, 1992). Because levee projects have the potential to dominate these high visibility landscapes, planting is often desirable, particularly in locations such as at and along major thoroughfares, parks, and waterfront developments (USACE, 2009).

Shields and Gray (1992) found that maintenance standards that allow woody shrubs and small tree growth on levees would enhance the structural integrity of sandy

levees. Similarly, Allen (2003) indicated that woody corridors between riverbanks and primary levees played a significant role in the reduction or prevention of flood related damage to levees.

While those studies point out that riparian trees increase levee stabilities, they could possibly cause several problems. For instance, proper vegetation managements on/near levees are needed for retaining accessibility for maintenance, inspection, monitoring, and flood-fighting. USACE indicates tree roots potentially penetrate levees and their drainage systems, which eventually cause seepage and piping. The vegetation-free zone also prevents structural damage resulting from a wind-driven tree overturning.

The USACE developed guidelines to assure that landscape planting and vegetation management provide aesthetic and environmental benefits without compromising the reliability of levees. A key feature of these guidelines is to have a vegetation-free zone is a three-dimensional corridor surrounding all levees (USACE, 2009). The vegetation-free zone applies to all vegetation except grass.

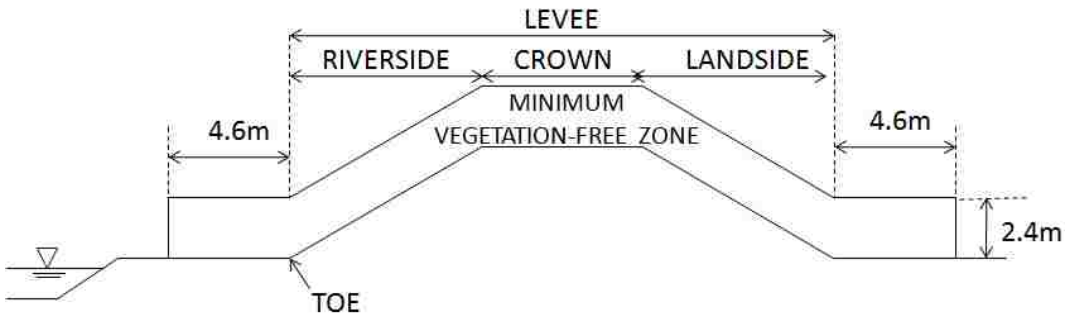

Figure 1.1 Vegetation-free zone defined by USACE (after USACE, 2009)

The primary purposes of the vegetation-free zone are to;

- Provide a corridor of access to levees for maintenance, inspection, and surveillance.
- Provide distance between a levee and root systems.

1.2 Overview of the preliminary work

As described in 1.1, riparian trees have the potential to degrade the levees as their roots extend under the levees. Vertical root barriers are one treatment that has been found to redirect root growth to lower levels of the soil, thus reducing damage to the sidewalk (Costello et al. 1997). The root barriers may allow trees to grow near the levee without compromising levee stability. Geosynthetics are frequently used as root barriers in various drainage designs (AVSR et al, 1994).

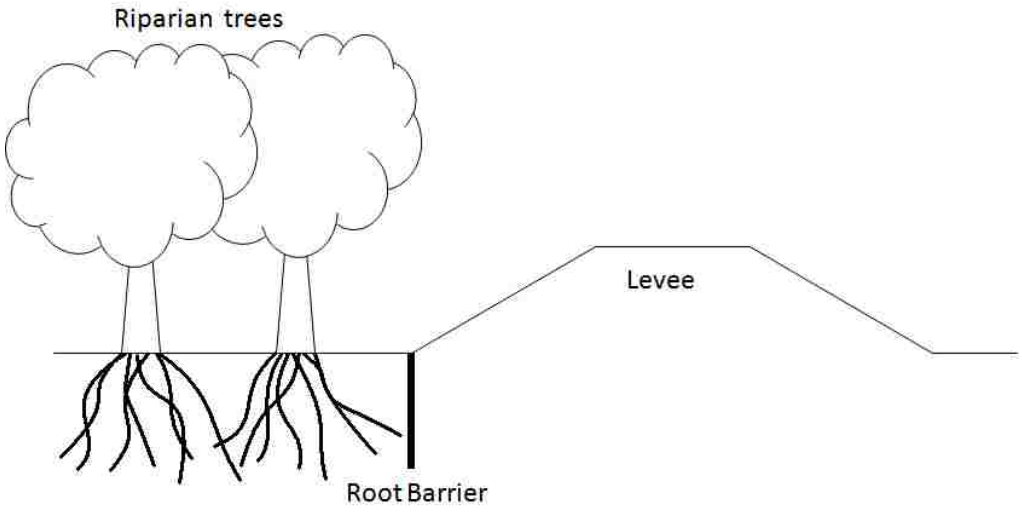

Figure 1.2 Example of root barrier installation near the levee

As levee performance may be enhanced by installing the root barriers adjacent to levee drains, evaluating the effectiveness of root barriers is crucial. Therefore, the preliminary work was aimed at determining the types of root barriers that might be most appropriate for arid region. The preliminary work consisted of three parts: determining the current state-of-practice for vegetation barriers, characterization of roots at representative sites in the Rio Grande Bosque and a bench-top experiment.

For the first study element, determining the current-state-of-practice, literature reviews were conducted to understand how geosynthetics were used as root barriers.

Also, cost and physical properties of several types of geosynthetics were compared. A summary of this comparison is found in 1.4.2.

Characterization of roots with a trench profile method revealed the presence of root systems in the levee structure. It showed that sandy soil had fewer large roots and clay-rich soil had more small roots. This suggests that when roots encounter high moisture content soil, they stop growing long and proliferate small uptake roots. When they grow through moisture poor soil, they just continue to extend. The intensive works required for root counting limited observation points into only three small areas. Research that is more comprehensive is needed to understand effect of roots on the levees in the entire riparian forest.

Also, the bench-top experiment showed the ability of the root barriers to prevent root growth of cottonwood and salt cedar, but one type of root barriers was broken by willow roots. Results from some preliminary tests are described in 1.4.2. Further experimentation is needed to better understand root growth in response of the application of the root barriers.

1.3 Purpose and scope of the study

The primary purpose of this study, which was designed based on the preliminary research, was to explore a method in assessing tree root encroachments on levees and their drainage systems.

Three research elements were undertaken in this study. First, ArcGIS and aerial photographs were used to assess the potential for root intrusion into levees in the MRG. Simultaneously, a bench-top experiment was conducted to test the root growth behavior in response to root barriers. Finally, a numerical model of saturated/unsaturated water

flow was developed to understand soil water movement in the levee structure under different conditions. The details of each element are explained in each section.

1.4 Literature Review

1.4.1 Estimating tree root encroachment on levees

With most engineering structures involving soils, levees are normally designed without consideration of effects of vegetation on soil properties (U.S Army Corps of Engineers, 1978). In recent years, increased environmental concern within construction agencies and greater responsiveness to public opinion have resulted in increasing numbers of levee projects designed, built, and maintained with environmental objectives in mind (Nunnally et al, 1987). Shields and Gray (1992) found levee maintenance standards that permit woody shrubs and small trees would provide greatest environmental resources benefits and would enhance structural integrity without hazards associated with large trees such as wind-throwing. However, according to the guideline for vegetation management on levees published by USACE (2009), currently only grass species are permitted to grow on the levee. While the importance of riparian vegetation for water quality management, aquatic habitat, and stream restoration is widely acknowledged, the impacts of vegetation on hydraulic structures are complex, poorly understood, and have yet to be fully quantified (Mosley, 1981; Murgatroyd and Ternan, 1983; Hickin, 1984; Heede and Rinne, 1990; Thorne et al., 1997; American Society of Civil Engineers, 1998a; Abernethy and Rutherfurd, 2000).

For a better understanding of the effect of vegetation on levee, it is important to obtain root distribution data in Bosque. The trench profile technique is the most common method for root observation (Noordwijk, 2000). It provides visible results, and is

supposed be the most accurate method in characterizing root systems (Costa, 2000). However, it is not the best option for studies with large observation areas as it is labor intensive, time-consuming, and difficult to implement. Remote sensing techniques have been applied as an alternative method in understanding vegetation volume and biomass. Although remotely-sensed data have become the primary source of biomass estimation (Lu, 2005), their application in estimating root distribution is yet poorly developed. Root systems are invisible in remotely-sensed data, and their complex structures make the estimation process more challenging is spite of the conveniences of remotely-sensed data. Therefore, the first research element, GIS-based aerial photography analysis, explored a new method of resolving this conflict. Further background on this research is described in the chapter 3.

1.4.2 Bench-top experiment

Preventing excess pore water within levees is a crucial process in enhancing the levee stability. Drainage pipes are constructed to prevent soil saturation within levees so that the levees maintain their functionality. However, live tree roots are frequently found penetrating and clogging pipes (Marer, 1996), limiting their effectiveness in removing excess water.

Current research on subsurface drainage focuses on drainage material, namely envelopes (AVSR et al, 1994). The envelopes are the materials that completely surround a pipe, providing support and/or protection. Previous research has demonstrated that the soil geotextile filter system can be more effective than the conventional graded soil filter system (Murty et al, 1994).

Root barriers may be used to provide an added measure of assurance for the drainage system, but they should not be a substitute for adequate distance between plantings and root-free zones. Depending on the application, it may be undesirable for root barriers to retard groundwater or seepage flow. Some root barriers include herbicides to enhance effectiveness; these should be evaluated prior to use to assure against negative environmental impacts (USACE, 2009).

Common root barriers include water-impermeable geomembrane-based barrier, water-permeable geotextile-based barrier, and water-permeable herbicide treated geotextile barrier. Geomembrane type root barriers redirecte root growth near the barrier, while herbicide barriers suppress root growth (Smiley, 2002). Wilson and Lister (2002) conducted mid-term (6-year) trench insert experiments, in which trench breakout was discovered in trenches with a geomembrane. No root penetration was observed in trenches with water permeable root barriers. Typar and Biobarrier were used as the water permeable barriers. Both Biobarrier and Typar are composed of lightweight polypropylene. Biobarrier has nodes attached to the geotextile that release trifluralin, which is a widely used herbicide. In contrast, Typar is simply composed of geotextile with no chemical effect. The results here suggest that Typar performed as well as Biobarrier in providing sufficient protection against root penetrations without the need for the additional (chemical) barrier provided by the trifluralin. Typar is generally priced 70 to 80% less than Biobarrier.

In the preliminary work that proceeded the work described in this study, two native species Rio Grande cottonwood (*Populus deltoids* ssp. *Wislizeni*) and coyote willow (*Salix exigua*), and one non-native species, saltcedar (*Tamarix chinensis*) were

collected from Bosque. They were grown in clear acrylic chambers whose bottoms were sealed with four types of root barrier: Typar (4oz), Typar (6.5oz), Typar (8oz), or Biobarrier.

To compare root growth in each chamber, total root length in each chamber was calculated. The root length estimation method was the same as that described in chapter 3.

Although cottonwood was not affected by herbicides attached on Biobarrier, saltcedar was greatly inhibited by Biobarrier. Saltcedar length was higher in Typar treatments than in a control column without root barriers. Vegetation barriers may enhance saltcedar growth by holding in moisture. Willow roots broke through Typar (4oz).

Biobarrier suppressed saltcedar growth; nevertheless, it is less desirable to its high price in comparison with other types of geosynthetics such as geotextile.

Barrier type Product name	Unit	Geomembrane Water barrier 0.76mm	Herbicide-based Biobarrier	Geotextile Typar ($136g/m^2$)
Cost	$\$/m^2$	5.8	21.42	0.66
Puncture Strength	kg	42	18	21
Unit Weight	g/m^2	820	130	136
Permeability	sec^{-1}	–	0.7	3
Longevity	yr	20	15	10

Table 1.1 Root barrier comparison, preliminary work

As shown in Table 1.1, herbicide-based root barrier is far more expensive than other types of root barrier. A simple geotextile is much cheaper while it has similar properties as herbicide-based barrier. Hence, geotextile was selected to test its capability of preventing root growth in the experiments described here.

A geocomposite is composed of geotextiles and a geonet (Figure 1.3). The geonet create a space between geotextiles, which is called “air gap” and may disable roots from penetrating the geocomposite. The air gap also may limit unsaturated water movement, and thus create moisture-deficient environments which are in general less desirable environments for roots. Thus, geocomposite was also used for the experiment in order to assess if air gap would redirect root growth.

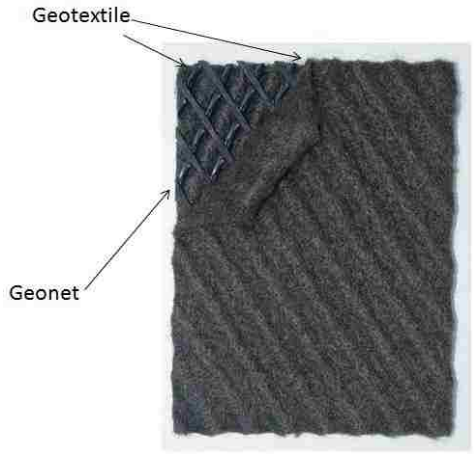

Figure 1.3 Geocomposite

The bench-top experiment was designed to test the ability of geotextiles and geocomposites to prevent root intrusion into drain facilities. Further information is found in chapter 4.

1.4.3 Numerical modeling

To evaluate the function of the levee and its drainage system, two-dimensional moisture movement (seepage) under and through the levee should be analyzed. Numerical models are a useful method to solve this problem, and HYDRUS-2D is a widely-used two-dimensional model for solving saturated/unsaturated vadose zone water movement (Simunek et al, 1999).

The levee on the west side of the Rio Grande between the Isleta Pueblo and the Pajarito neighborhood in Albuquerque's South Valley was reconstructed in 2009 based on hydrologic and geotechnical analysis (U.S. Army Corps of Engineers, 2008). AMEC utilized the new levee geometry and soil sampling data for developing numerical modeling to understand seepage through the levee (AMEC, 2008). They developed the model with a typical toe drain design used for the levee drainage system (Figure 1.4).

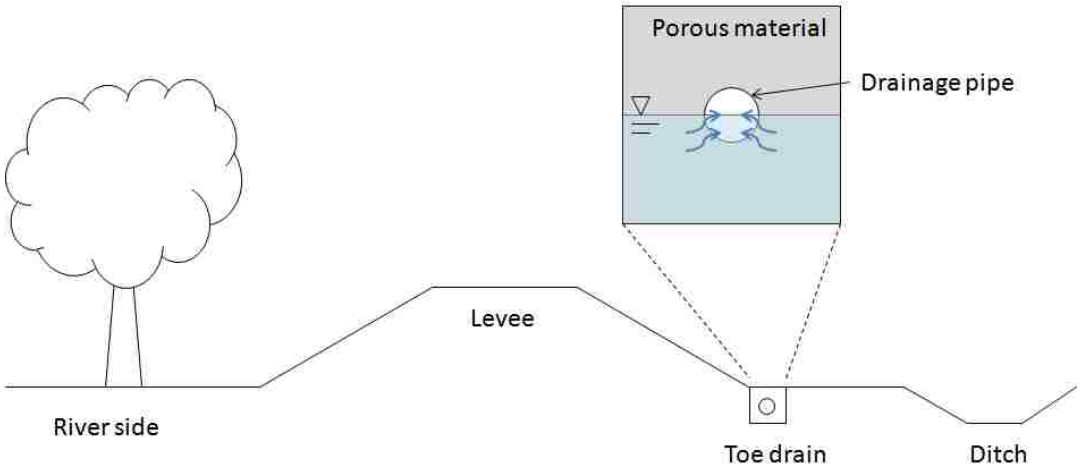

Figure 1.4 Toe drain

In the past 20 years, prefabricated geocomposite drains have become a common method of water drainage for a wide variety of purposes. In many cases these drains are cheaper, thinner, easier to construct, and require less space than conventional drains constructed using aggregate wrapped in a geotextile (McKean and Inouye, 2001). The voids within the geonet serve to replace the drainage pipe in a conventional toe drain (Figure 1.5). The geocomposite drain may become an alternative for the conventional toe drain. Therefore, drainage functions of toe drain and geocomposite drain were compared using the numerical modeling.

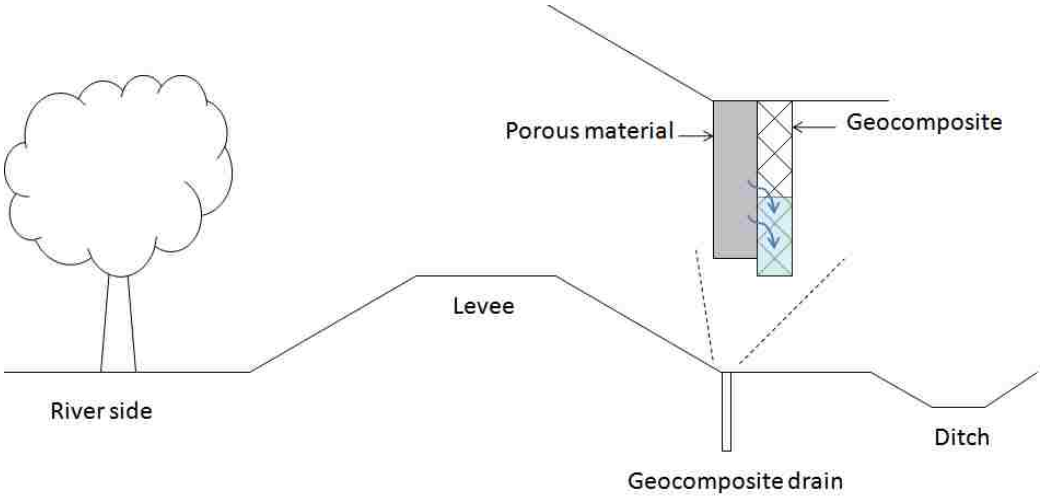

Figure 1.5 Geocomposite drain

CHAPTER 2: ESTIMATING TREE ROOT ENCROACHMENT ON LEVEES

2.1 Introduction

As described in chapter 1, it is necessary to consider the effect of vegetation roots when designing levees and their drainage system. In addition to a trench profile - technique, ground-penetrating radar is widely accepted for observing root systems. Despite of accuracy of their results (Stokes, 2002), they are time-consuming and laborious; therefore, study areas are very limited in most cases.

U.S. Army Corps of Engineers (USACE) published a guideline for vegetation management at levees (USACE, 2009), suggesting the use of tree crown size as an indicator of horizontal extent of root distribution. Crown size provides a general idea of root growth even though root growth differs by species and local environmental conditions such as water availability. Accordingly, this study was developed to estimate horizontal extent of root distribution using tree crown sizes.

There are several methods to measure tree crown size. To measure tree crown size in large areas, GIS-based data is widely used, and is gaining more popularity in recent years. For instance, airborne lidar was applied to measure individual tree crown sizes in the southeastern United States (Sorin et al, 2003). This investigation concluded that lidar data is a reliable tool in measuring tree crown sizes, thus improving estimates of forest biomass and volume. Although many studies have proven the possibility of lidar data to be used in a tree crown size analysis, preparation of a proper data set remains difficult. Lidar data sets need to be collected specifically for that purpose; for example, using multiple returns, and a low flying height. Even though several lidar data sets were tested to measure tree crown size in the riparian forest in MRG, it was impossible to obtain an

accurate result due to their poor quality for this application. Because it is important to develop an inexpensive method so that the effect of tree roots on levees can be easily considered before designing levee drainage system, required data for estimating tree crown sizes needs to be readily available.

Obtaining aerial photography is not difficult in contrast to lidar data. Accordingly, for this research, several aerial photographs were investigated to measure individual tree crown sizes. First, ArcGIS was applied to measure the locations and the crown sizes of the riparian trees adjacent to the levees in high-resolution aerial photography. These GIS-based measurements were verified against existing vegetation maps created based on field observations. In addition, readily available normalized difference vegetation index (NDVI) grids were compared with the aerial photography and the vegetation maps to evaluate the potential for NDVI to be applied for similar analyses. The type and size of vegetation was then used in models to predict the lateral extent of the root system to determine if the root system would impinge on the adjacent levee.

2.2 Method

Figure 2.1 shows procedure for crown size estimation. Details of each step are shown in the following sections.

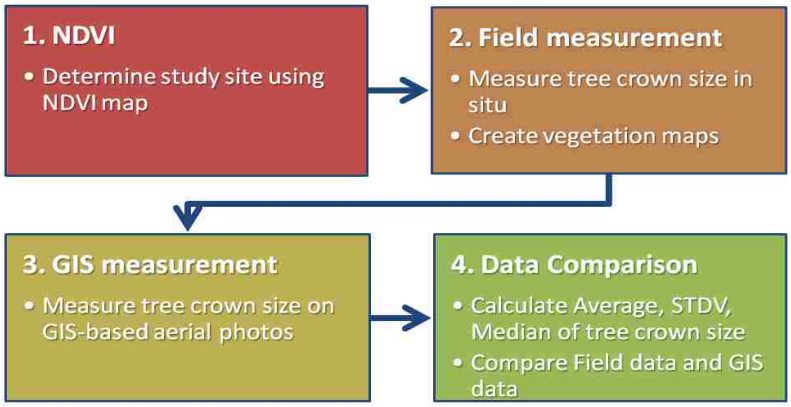

Figure 2.1 Procedure for crown size estimation

2.2.1 NDVI data

The Normalized Difference Vegetation Index (NDVI) is a simple indicator of vegetation greenness derived from data from two satellite channels: near infrared (NIR) and red.

$$NDVI = \frac{NIR - red}{NIR + red} \quad (2.1)$$

NDVI thus takes values ranging from –1.0 to +1.0. Positive NDVI values indicate vegetated surfaces, and higher values indicate increasing density of green vegetation. Reflectance of the red portion of the spectrum decreases as solar radiation is absorbed, largely by chlorophyll, whereas reflectance of the near infrared portion is caused by leaf mesophyll structure (Kremer and Running, 1993). Negative NDVI values indicate non-vegetated surfaces such as water, ice, and snow (Weiss et al, 2003)

McDonnell (2006) utilized NDVI to identify the vegetation type along the Middle Rio Grande corridor using Landsat 7 ETM+ imagery and the decision tree classifier (DTC). Images were acquired for the 2001 and 2002 growing seasons (May to September). Decision tree classifier methodology was applied to perform multistage classification based on “yes” or “no” answers to expressions or rules about NDVI values. The final decision trees evolved after several iterations and the final field verification. Finally, the study site was classified into thirteen areas with different types of vegetation: *Populus deltoides* (cottonwood), *Elaeangus angustifolia* (russian olive), *Tamarix chinesis* (saltcedar), *Salix exigua* (sandbar or coyote willow) and other scrubs, scrub grass mix, grasses, low density agriculture, moderate density agriculture, high density agriculture, sand and non vegetated areas, shallow water/wetlands, irrigation, river and lakes.

On these NDVI grids, if an area was classified as “cottonwood”, it would have not only cottonwood trees, but also understory species which grow under cottonwood crowns. It was impossible to detect what was growing under tree crowns with the NDVI data. In contrast, if an area were classified as other vegetation types, for instance, willow, it would be covered only with willows.

2.2.2 Study sites

On NDVI map, dominant species near the levee were cottonwoods and/or willow, so two study sites which is mostly covered with those two species were selected (Figure 2.2). As cottonwoods and willows are very common New Mexican species, only those two species are referred in this study, and other species are not discussed. The first study site, Site-A, is located south of Alameda Bridge (35° 11' 18.0"N, 106° 38' 45"W), which is covered with cottonwoods and willows (35° 5' 34.8"N, 106° 41' 6"W) according to the NDVI map. The second site, Site-B, is located north of Central Bridge, and covered with mainly cottonwoods.

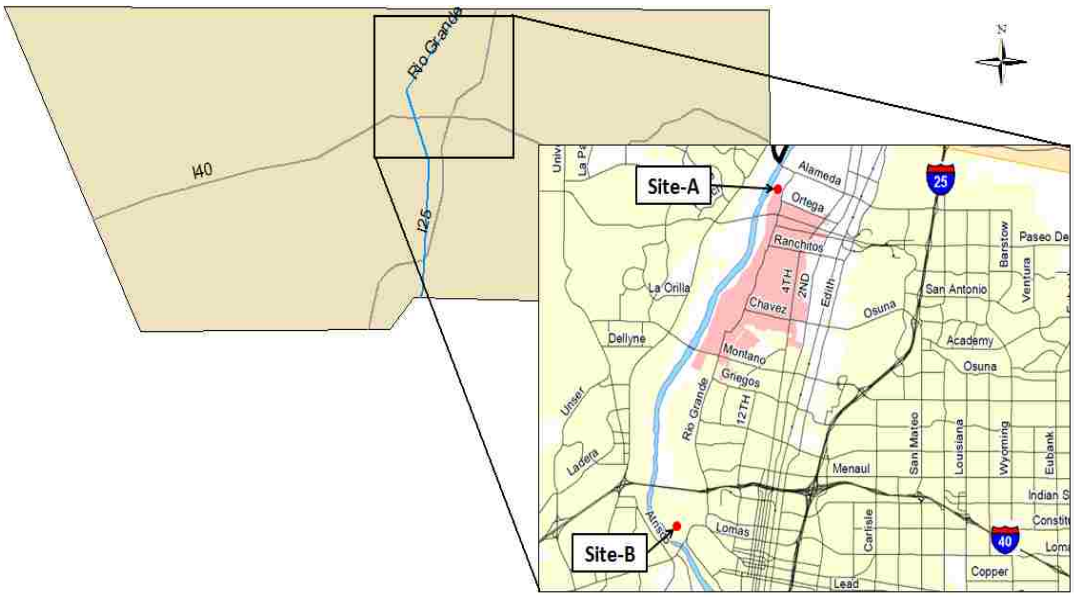

Figure 2.2 Study sites

2.2.3 GIS-based crown size estimation

2.2.3.1 Aerial photograph

Three different types of aerial photographs were used to measure the tree crown sizes: Natural color, RGB (Red, Green, Blue), and CIR (Color Infrared) as shown in Figure 2.3.

Figure 2.3 Aerial photographs

- Natural color aerial photography

The photographs that depict color digital aerial photographs were acquired in the spring of 2008 prior to leaf-out conditions. The Bernalillo County GIS Program provides high-resolution (2.54 cm x 2.54 cm) aerial photography with natural color to public with no charge. Although the natural color images have good resolutions, it appears as though camera tilts have not been removed. As shown in Figure 2.4, some trees appear to be overturned due to the camera tilt effect. Also, it is difficult to measure crown size on those images as they were collected during the leaf-off season.

Figure 2.4 Natural color aerial photography. Note that the trees seem to be inclined as camera tilts have not been removed.

- A Digital Orthophoto Quarter-Quadrangle (DOQQ) (RGB and CIR)

DOQQ is a computer-generated image of an aerial photograph in which image displacement caused by terrain relief and camera tilts has been removed. Two kinds of DOQQ were downloaded from New Mexico Resource Geographic Information System Program's website (http://rgis.unm.edu/intro.cfm): RGB and CIR. RGB data is organized in three color bands or channels representing the red, green, and blue (RGB) portions of the spectrum while CIR (Color Infrared) is organized mainly with infrared. Camera tilts, which were problematic on natural color photography, were removed in RGB and CIR photography; however, the DOQQs were produced with resolution of 1 m, which is coarser than the resolution of natural color imageries. Therefore, the DOQQs were

compared with the natural color photography so that more precise measurement could be accomplished.

2.2.3.2 Tree crown size measurements on aerial photographs

ArcGIS provides a measurement tool, enabling users to measure directly distance and/or length on GIS maps. Using the measurement tool, the individual tree crown sizes and their locations were measured on the aerial photographs imported into ArcGIS.

Crown sizes were measured twice per one tree crown. The shortest spread and the longest spread were measured to calculate the average value.

2.2.3.3 Estimation of lateral root extent

The U.S. Army Corps of Engineers suggested estimating minimum horizontal extent of tree root system (USACE, 2009), using the following relationship:

$$Tree\ crown\ radius\ \times 1.75 = Horizontal\ extent\ of\ root\ system \quad (2.2)$$

The equation was developed for the trees in medium to large size. The USACE does not substantiate this formula with any data in the guideline where this formula is suggested. To evaluate this formula, literature reviews were done regarding tree root growth. However, only few studies have been undertaken on root system due to its complexity, and there is not sufficient literature to evaluate the formula. The formula was discussed by contacting experts in this field (Dr. James Cleverly, Research fellow at the University of Technology, Sydney; Dr. Clifford Crawford, Research Professor at the University of New Mexico; Mr. Nick Kuhn, Albuquerque City Forester, Gordon Mann; Consulting Arborists at Mann Made Resources). They pointed out roots grow where the conditions are suitable. For example, root growth would vary with water availability, health, soil type, site conditions, and management. One simple formula would not be

capable of accurately judge root growth. Some experts mentioned that if the formula was applied from a tree trunk, horizontal extent of root system might be underestimated.

The original USACE formula was applied in this study to estimate minimum possible root extent in the riparian forest.

2.2.4 Field observation and vegetation mapping

Individual tree crown sizes were measured at the Site-A and Site-B. As shown in Figure 2.5, the width of a crown can be measured by projecting the edges of the crown to the ground centre. The longest spreads and shortest diameters were measured to calculate average crown sizes. Locations of trees were also obtained with GPS units. Vegetation maps were created based on collected data.

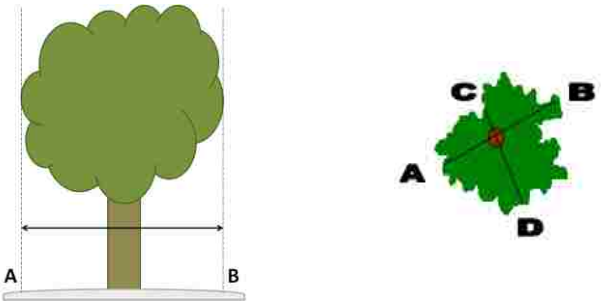

Figure 2.5 Tree crown size measurement

2.3 Results

2.3.1 Site-A

At Site-A (Figure 2.6), which is covered mostly with cottonwoods and willows, it was very difficult to measure individual tree crown sizes due to its complex vegetation community. On the vegetation map (Figure 2.7), it appears as though most understory species grow underneath the cottonwood crowns. However, as the vegetation map was created with average crown size, the actual vegetation coverage and crown shape are not

identical to the vegetation map. At Site-A, three cottonwood trees were found in the field measurements, and they had complex crown shapes rather than simple circles. In reality, understory species such as willows were not completely overlaid by cottonwood crown. Siberian elm is not discussed here as it is minority species.

Even though willows are visible on the aerial photographs, the resolution of the photographs was not fine enough to measure small willow crowns. As the field measurement indicates, the average crown size for willow is 0.64 m (Table 2.1). The natural color aerial photography has resolution of 2.54 cm. Despite the fact that the average crown size is lager than the resolution, the photography has camera tilts which make measurement more difficult. In contrast, resolution of RGB and CIR photography was too coarse for the measurement of willow crown size. Consequently, none of the photography was appropriate for the GIS-based crown size measurement for Site-A.

Table 2.1 and 2.2 include estimates of the horizontal extent of root system using the USACE equation (Equation 2.2) for willows and cottonwoods, respectively. In total, 21 willows were found at the site. Estimated horizontal extent of the willow root system was 1.13 m in average. As most willows were not found near the levee, they are unlikely to threaten the levee drainage systems. Also, only average crown size is given here. In contrast, as shown in Table 2.2, all root systems of cottonwood are estimated to reach the levee line since the estimated horizontal extents of their root systems were longer than distance between the levee and each tree. Distance between an average cottonwood crown radius was not calculated as only three cottonwoods were found, and their size greatly varied.

Figure 2.6 Natural color aerial photograph for Site-A

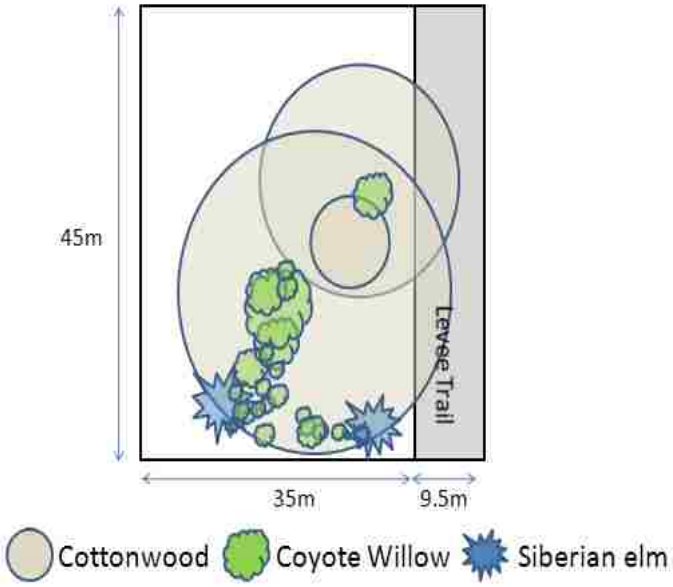

Figure 2.7 Vegetation map, Site-A

Table 2.1 Average crown radius for all willow, Site-A(Unit: m)

	Average crown radius (CR)	Horizontal extent of root system, CR x 1.75
Average	0.64	1.13
STDV	1.14	1.26
Max	1.55	2.71
Min	0.23	0.39
Median	1.1	1.32

*21 Willows were found in total

Table 2.2 Average crown radius for individual cottonwood, Site-A (Unit:m)

No.	Distance between Levee and tree trunk	Average crown radius CR	Horizontal extent of root system CR x 1.75
1	7.2	11.0	19.2
2	5.7	3.3	5.7
3	3.7	7.9	13.7

2.3.2 Site-B

In contrast to Site-A, Site-B has simple vegetation community with cottonwood and fewer understory species. Understory species are mostly found underneath the cottonwood crowns; thus those understory plants are not visible on the aerial photography. Tree crown sizes were measured on the aerial photography with the ArcGIS measurement tool. In the field measurements, 8 cottonwoods were found in total. Table 2.3 shows the comparison of two measurement methods. The GIS-based average crown radius was 1.22 m larger that of field measurement. It appears as though shade and camera tilts made it difficult to distinguish the edges of tree crowns. The difference in estimated tree crown size resulted in a 2.13 m difference of the horizontal extent of root system. Although small cottonwoods were not detected on the GIS-based measurement it is more important to understand the root systems of larger trees as they would be

expected to be larger, and likely have a greater horizontal extent. Thus, at this site, the GIS-based measurements provided a reasonable estimate of tree crown radius. Using equation 2.2, four cottonwoods have root systems that reach the levee.

Figure 2.8 Natural color aerial photographs for Site-B

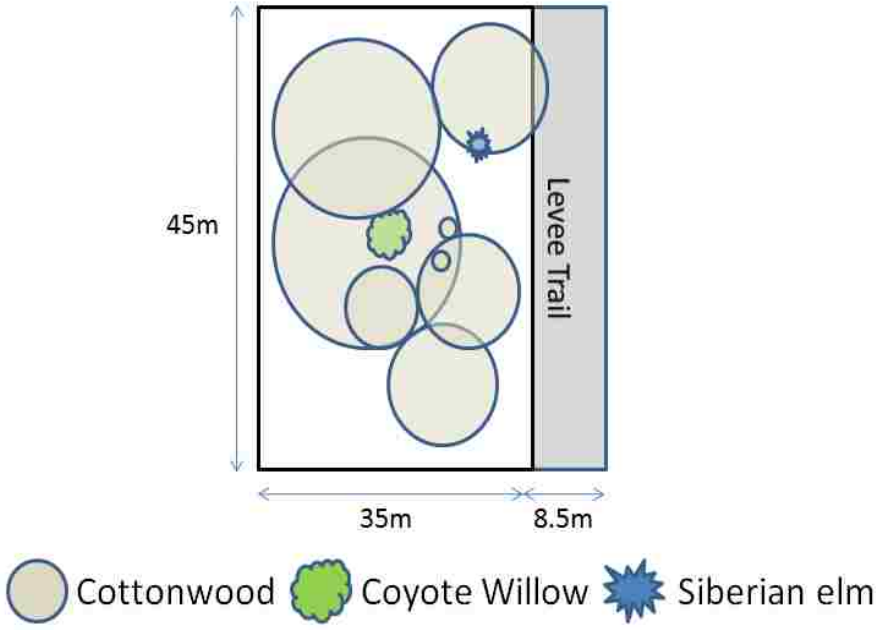

Figure 2. Vegetation map, Site-B

Table 2.3 Average crown size, Cottonwood, Site-B (Unit: m)

	Field measurement		GIS-based measurement	
	Crown radius	Root system	Crown radius	Root system
Average	5.35	9.36	6.57	11.49
STDV	3.41	5.97	3.36	5.89
Max	10.35	18.11	12.09	21.15
Min	0.93	1.62	2.55	4.47
Median	5.68	9.93	5.83	10.2

Table.2.4 Crow radius of each Cottonwood and their horizontal extent of root system, Site-B (Unit: m)

No.	Distance between Levee and tree trunk	Crown radius (CR)	Horizontal extent of root system CR x 1.75
1	9.5	4.73	8.27
2	8.2	4.10	7.18
3	9.0	4.50	7.88
4	10.6	5.30	9.28
6	4.1	2.05	3.59
13	19.9	9.95	17.41
14	17.9	8.95	15.66
16	16.5	8.23	14.39

2.4 Conclusion

2.4.1 Major findings

Although high-resolution aerial photographs were used, measuring tree crown size remains difficult due to the resolution. Also, complexity of the forest reduces the accuracy of the estimation. For instance, only overstory can be observed from satellite image and aerial photography, and understory species such as willow cannot be detected. Thus, in Site-A, which is covered with many shrubby species such as willow, crown sizes were not able to be measured on the aerial photographs. However, as root system of shrubby species is probably not large enough to threaten the levees, it is likely that there

is no need for measuring their crown sizes. In contrast, the GIS-based measurement showed a reasonable comparison to field measurements at Site-B with its simple vegetation community.

The measurements and observations reported here suggest that GIS-based measurements have the potential to be used to estimate root encroachment on levees, especially for sites with simple vegetation communities. Suggested improvements in GIS-based measurement methods using aerial photography include removing shade and camera tilts effect.

With respect to the field observation, several cottonwoods were found near the levees, and their estimated root length would reach the levees and their drainage systems. Even though field observations can be performed in limited areas due to time constraints, field observations remain the preferred method to estimate influence of vegetation roots on levees.

CHAPTER 3: BENCH-TOP EXPERIMENTS

3.1 Introduction

In the preliminary work, bench-top experiments were conducted to evaluate the effectiveness of two types of root barriers: a simple geotextile and an herbicide-based barrier. While the herbicide-based geotextile can be effective as a root barrier, these materials are more expensive than conventional geotextiles. Thus, the bench-top experiment described here was designed to test the ability of conventional geotextiles and geocomposites in preventing root intrusion into drain facilities. These materials are often used as filters. The objectives of this experiment are to evaluate the effectiveness of these geosynthetic materials as root barriers. In particular, it is important to know whether or not root penetrate through the barriers. Differences in root growth in response to different types of barriers and drainage material are evaluated.

3.2 Methods and Materials

The bench-top experiments were conducted to evaluate the effectiveness of two types of geosynthetic materials as root barriers. A geotextile and a geocomposite were tested in clear columns filled with soil and/or gravel simulating six different drainage designs. Two New Mexican native plants, Rio Grande cottonwood (*Populus deltoides ssp. wislizeni*) and coyote willow (*Salix exigua*), were selected, and planted in the columns. After a five month growth period, total root length was measured in each column to evaluate the effect of barriers on root growth.

3.2.1 Plant collection and preparation

Rio Grande cottonwood (*Populus deltoides ssp. wislizeni*) and coyote willow (*Salix exigua*) were selected as they are native New Mexican species. Inflorescences of cottonwood and coyote willow were collect from nearby the Rio Grande, approximately

1.5 km north of the Central bridge (106°41′36.55″W, 35°06′04.54″N). The inflorescences were stored in a paper bag for one week until they released fruits, which were then placed on wet paper towel for germination. After they germinated, they were transplanted into small pots to prepare seedlings. After they grew to the height of 10 cm, they were transplanted into experimental columns.

3.2.2 Experimental columns and root barriers

The schematic design of an experimental column is shown in Figure 3.1. The bottom of the 30 cm long, 10.16 cm diameter acrylic tube was enclosed with acrylic sheet. The valve was attached on sidewall near the bottom so that a water table could be controlled in each column. Root barriers were inserted into the column horizontally at the height of 10 cm from the bottom lid. As a root barrier, two conventional geosynthetic materials were used: a geotextile ($4oz/yd^2$) and a geocomposite (double-sided, 4 oz geotextile with 2 mil geonet). Detailed information about root barriers are given in Appendix A.

The upper parts of the columns were filled with sandy soil that was obtained from bosque obtained from the same location as the inflorescences. Two types of drainage material were used to investigate the root growth response with different drainage materials. In addition to sand, gravel was prepared as a drainage material to test whether the expected lower saturations and the larger voids (air gap) within gravel would prevent or limit root intrusion. Since root tends to grow proliferate in areas with higher moisture content, root growth may be stopped when root meets air gap with little or no water. The detailed description of drainage material and their placement are shown in Appendix-B. Being developed with different conventions of root barriers and drainage materials, there

were six combinations per species. Three replicate columns of each combination were constructed for two species, totaling 36 columns (Table 3.1).

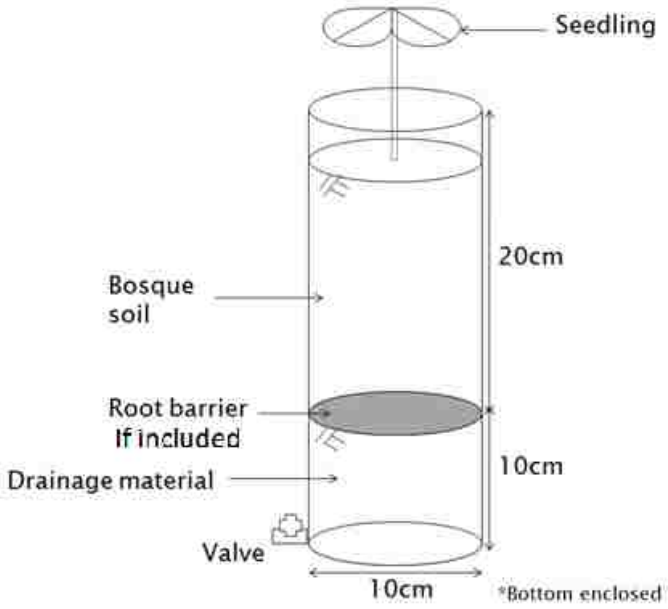

Figure 3.1 Schematic of experimental column

Figure3.2 Photograph of experimental column

Table 3.1 Matrix of column configuration

Barrier	Material in the bottom (drainage layer)	Plants	
		Cottonwood	Willow
Control (no barrier)	Soil	3	3
Control (no barrier)	Gravel	3	3
Geotextile	Soil	3	3
Geotextile	Gravel	3	3
Geocomposite	Soil	3	3
Geocomposite	Gravel	3	3

*Total 36 columns

3.2.3 Experimental condition

During the five-month growing period, the water table was controlled through the attached valve. For the first three months, water table was maintained 10 cm below the soil surface to encourage plant growth. The water table was then lowered to 25 cm (1cm/day) from surface to induce further root growth into the lower portions of the columns. A 1000W metal halide bulb lit the plots for 13 hours per day. The metal halide bulb has a strong blue spectrum, which promotes short stocky vegetative growth. The light was set 1 m above the soil surface.

3.3 Data analysis

3.3.1 Newman technique

After the five month of growth period, the columns were disassembled for measurements of the roots. The total root length was estimated using the root length estimation method developed by Newman (1966). Total length of a root system (any set of curved lines) is proportional to the number of intersections (N) formed with the perpendicular lines given the surface area (A) of the container and the total length of straight lines (H) (Wilhelm et al, 1983):

Where

$$R \propto \frac{N}{2H} \quad (3.1)$$

R= estimated root length

N= number of intersections between roots and lines (total)

A= area in which the roots are spread out

H= total length of lines used

3.3.2 Procedure

After disassembling the pots, roots were carefully collected from the top and bottom portions of the column. The roots were then washed, and the secondary roots were cut off from the main roots to make roots spread out on a clear container with minimal overlapping. Next, the clear container was placed on a light table with grid to take photographs. The photographs were imported to image analysis software (Image J 1.43). To count the number of intersections between roots and lines (N in Equation 3.1), 16 lines in equal numbers of rows and columns) were selected using the random number

generator function in Microsoft Excel. The results were then used to calculate the total root length in the column.

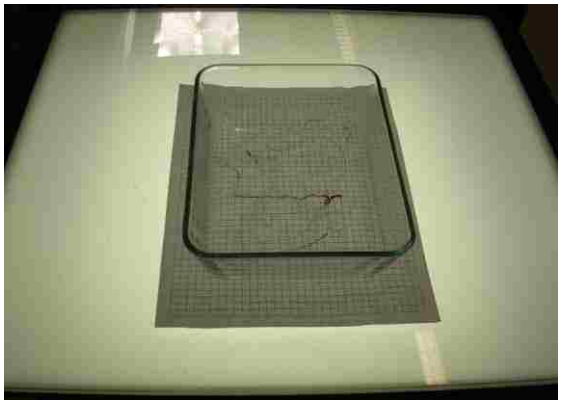

Figure 3.3 Clear container on light table

3.4 Results

3.4.1 Cottonwood

In all columns, root systems were found not only in the upper parts of the column, but below the root barrier as well. Thus, the root barriers were not effective in preventing root growth, and allowed roots to grow into the drainage materials. A photograph of root penetration is shown in Figure 3.4. Total lengths of root systems greatly differed in each column. Although they were grown under the same conditions, their growth was not identical; accordingly, very large standard deviations were obtained (Figure 3.5). As mentioned in 3.2.2, three columns were prepared with same combination of the root barriers and the drainage materials to calculate mean value. However, in the middle of the five-month growth period, some plants died for unknown reasons, resulting in a sample size of one and zero standard deviation.

Figure 3.6 shows the percentages of root length in the upper and lower chambers. There are no apparent differences between control columns and those with different root

barriers. Thus, Figure 3.5 and Figure 3.6 indicate that regardless of the root barriers or drainage materials, roots grew through the root barriers.

Even though the water table was lowered to create air gap, roots can continue growing through gap in response to gravitropism and thereby breaking through the root barriers. The estimated total root lengths seemed to be unrelated to the drainage material or root barriers. After bridging the gap to the water table, root proliferation generated a full root system and equalized root growth in upper and lower chambers.

Figure 3.4 Photograph of root growth through geotextile

*The drainage material was sand, and the root barrier was the 4 oz geotextile.

Table 3.2 Description of labels in Figure 3.5 to 3.8

Label	Drainage Material in the bottom	Root barrier
Control_sand	Sand	No root barrier
Geotextile_sand		Geotextile
Geocomposite_sand		Geocomposite
Control_gravel	Gravel	No root barrier
Geotextile_gravel		Geotextile
Geocomposite_gravel		Geocomposite

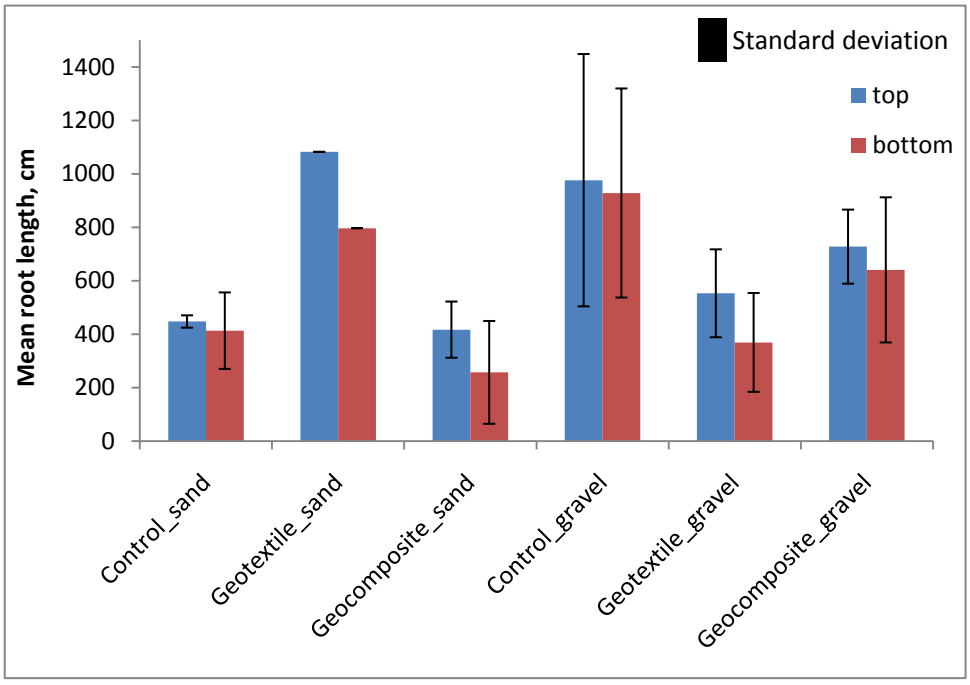

Figure 3.5 Average total root length and standard deviation (cottonwood)

*Top: root systems collected from the upper columns

Bottom: root svstems collected from the bottom columns

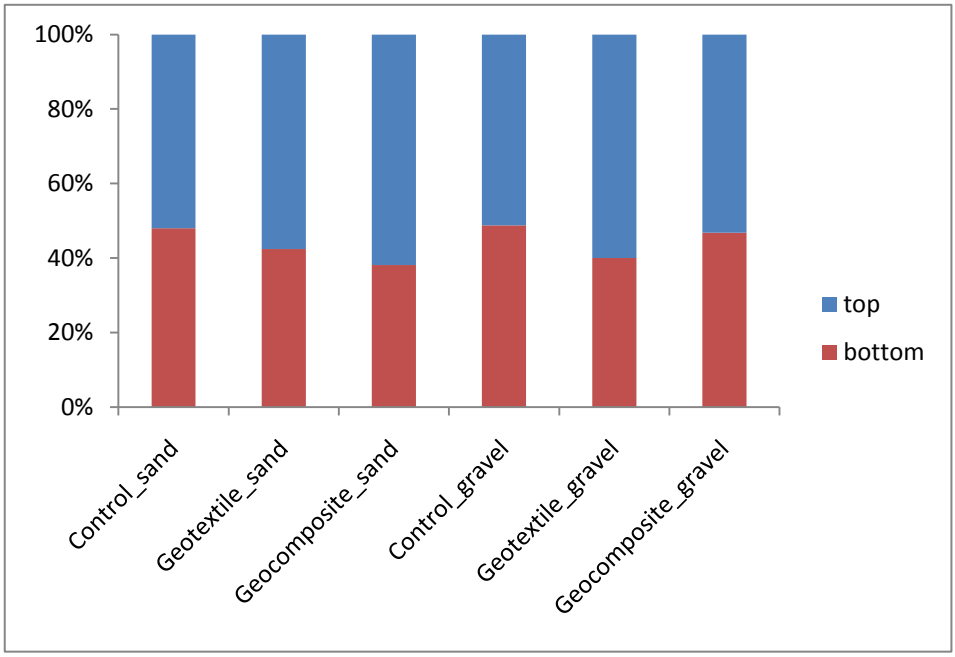

Figure 3.6 Percentage of root length in the upper/lower columns (cottonwood)

As shown in Figures 3.7 and 3.8, root systems are found in all lower columns and the drainage materials and root barriers does not appear to affect the total root length of willows. The numbers of surviving columns made it more difficult to draw conclusions. There were two principal reasons for the low survival rate.

First, some willows died as happened for cottonwoods after they were transplanted into the columns. Survivability rate did not appear to be related to the root barriers or the drainage materials.

The second reason for low survivability is that some roots did not grow into lower columns. In many columns, some roots grew between the root barrier and the column wall (Figure 3.9). As willow roots are much finer than cottonwood, some root found a small gap along the column wall and the root barrier. When the columns were built, 30 cm of acrylic columns were first cut into two pieces to insert the root barriers, and they

were connected with glue and clear tape. Some roots broke through those joints, avoiding growing through the root barriers. Columns where roots broke through the joints were excluded from the statistical analysis because results would not show accurate total root length in lower chambers.

Although water table was lowered during the last two month of growth period, it was raised periodically so that soil in the upper columns did not get extremely dry. It was necessary because willows tended to die when the soil in the upper columns became very dry. The water table was immediately lowered after it moistened the upper portions, but it is conceivable that a small amount of water stayed between the clear tapes that were used to join the upper column and the lower column. Willow roots likely have smaller power to penetrate through root barriers due to their small size compared with cottonwood. Consequently, when they hit the root barriers, they grow outside of the columns where moisture was captured in the transparent tapes.

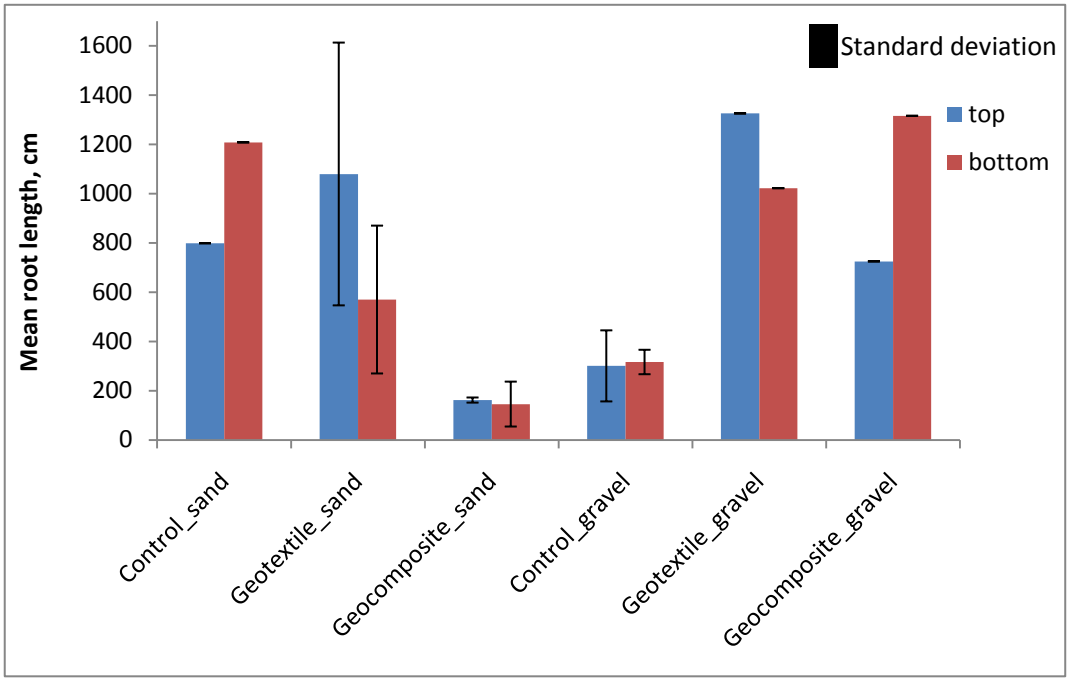

Figure 3.7 Average total root length and standard deviation (willow)

*Top: root systems collected from the upper columns

Bottom: root systems collected from the upper columns

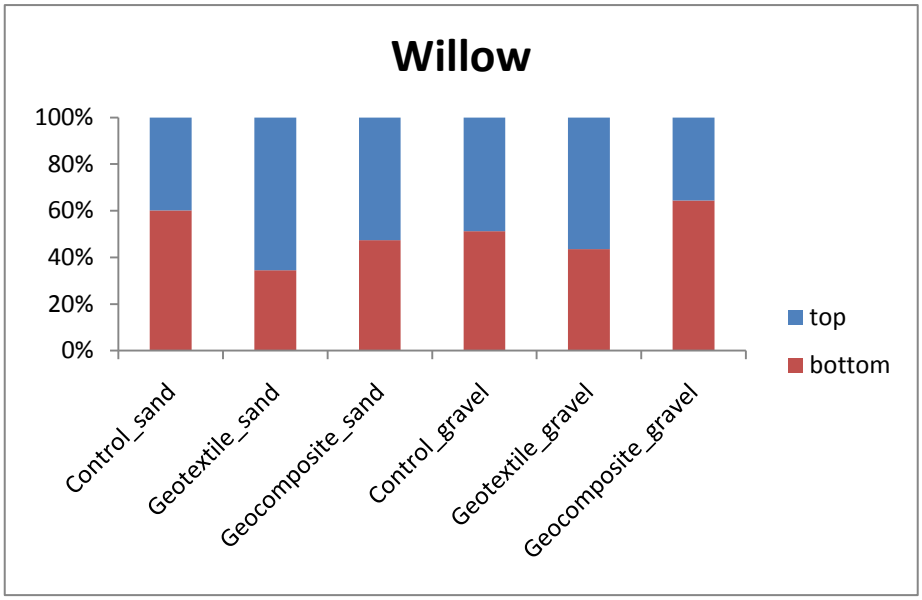

Figure 3.8 Percentage of root length in the upper/lower columns (willow)

Figure 3.9 Picture of root system grow found outside of the column

3.5 Conclusion

3.5.1 Major finding

Root systems of cottonwood and willow penetrated through the geocomposites and the geotextiles, thus, these experiments provided no evidence that these materials have any benefit in limiting or preventing root growth for these species in this configuration. Also, root growth was not dependent on the material beneath the root barrier (sand or gravel). While cottonwood roots penetrated barriers without exception, willow roots tended to find a path between the root barrier and the column.

Some fine soil accumulated in the gravel filled lower chambers. As fine soil can retain more moisture than gravels, roots might have more substrate in which to proliferate near the water table. Two possible reasons for the fine soil are; first, it was washed down from the upper parts of the columns due to their small particle size which could flow through the root barriers; second, it was associated with the gravel material itself.

3.5.2 Suggestions for further research

Modifications to the experimental system may improve figure results. The experimental columns should be larger. The thin upper layer (20 cm thick) in the columns may be insufficient to sustain a root system without it being motivated to grow deeper. Sample size should be increased due to seeding attrition. Also, a piece of geotextile should be larger, and sides of the upper chamber should be run up. In addition, a better connection between the root barrier and the sidewall would be helpful to keep small roots from bypassing the root barrier. Finally, an alternative configuration where the root barriers are evaluated for limiting horizontal rather than vertical root growth would be insightful.

CHAPTER 4: NUMERICAL MODELING

4.1 Introduction

The principal motivation for levee drainage is to increase the stability of the levee. It is important that water entering levee systems is drained as fast as possible. Levees are frequently constructed with horizontal toe drains from which excess pore water be drained. Drainpipes may become clogged by siltation, by chemical deposits (mainly iron oxides) and by root penetration (Dierickx, 1993). Presumably, this root growth is in response to favorable conditions in the drainage materials including moisture. It is important to understand where soil has higher moisture content so that future root proliferation can be estimated. In this study, a two-dimensional analysis of soil water movement through a levee with a horizontal toe drain was conducted. The main purpose of this study is to estimate soil water movement in response to weather events and flood water so that drain performance can be estimated, and the potential for proliferation can be estimated. In addition to a conventional toe drain featuring a gravel filled trench and a perforated pipe, a geocomposite edge drain configuration was modeled. The HYDRUS-2D computer program was used for this analysis.

4.2 AMEC report

Input data for the models was mainly obtained from Albuquerque West Levee Project Geotechnical and Seepage Analysis Report by AMEC Earth &Environmental, Inc. (AMEC, 2008). Soil and sediment sampling data was used to perform seepage and slope stability analyses of the proposed levee geometry. Seventeen cross sections in West Levee Project site at approximate 300 m spacing were analyzed with VS2DT, a computer

program that solves water/solute movement in vadose zone. In each cross section, soil hydraulic parameters (Table 4.3) and levee geometries were described in addition to their simulation results. The levee geometry and soil hydraulic parameters used by AMEC were used in this study. They created models with the conventional toe drain configuration. In this study, models were created with the geocomposite edge drain in addition to the toe. They analyzed seepage under flood conditions with no precipitation or evaporation. In contrast, in this study, precipitation and precipitation data was applied under no flood conditions, specifying different boundary conditions.

4.3 Project summary

Models of typical levee geometries were created using HYDRUS-2D. Hydrus-2D software was originally developed and released by the U.S. Salinity Laboratory in cooperation with the International Groundwater Modeling Center (IGWMC), the University of California Riverside, and PC-Progress, Inc. It was developed for simulating water, heat, and solute movement in two-dimensional saturated/unsaturated media. To begin, a model using ambient conditions with no climate data was run for 6000 days to obtain an initial equilibrium condition that would be used as the initial condition for subsequent simulations. Although most parts met equilibrium condition within 100 days, one small area with a low hydraulic conductivity required long time to reach equilibrium conditions. The final pressure head distribution from this simulation was then imported as the initial pressure head condition for two other models: one ambient condition and one flood condition.

Ambient conditions refer to typical conditions experienced by the levee. As there is no surface water impinging on the levee under ambient conditions, the levee will likely be unsaturated and there will be no drainage.

For flood conditions, surface flood water acts on the riverside of the levee. In this case, portions of the levee will likely be saturated; thus drainage is expected. Using these conditions, different drainage design can be evaluated.

The Hydrologic Engineering Centers River Analysis System (HEC-RAS) was used to calculate flood water depth in the flood condition (Figure 4.1 and Table 4.1). A 100-yr flood event was simulated. The details of HEC-RAS modeling are given in Appendix-C.

The Meshgen-2D module can be used to design boundary curves of virtually any two-dimensional computational domain in a MS Windows graphical environment (Simunek et al, 1999). The geometry of the levee was created with Meshgen-2D.

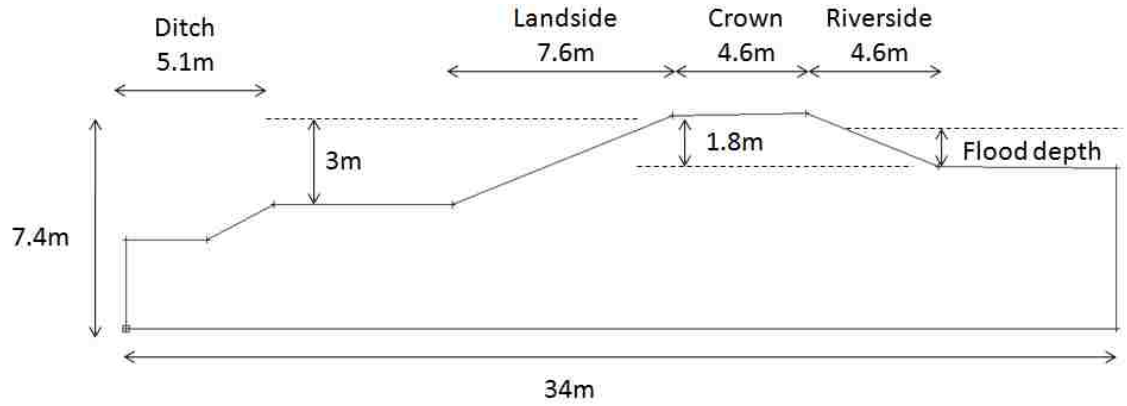

Figure 4.1 Flood depth at a levee

Flood event Exceedance probability,yr	flood depth m
2	0.29
5	0.41
10	0.57
50	0.90
100	1.06
200	1.21
500	1.45

Table 4.1 Flood depth in response to different flood event

4.4 Input data

In this section, various input data for HYDRUS-2D are described.

4.4.1 Geometry information

Geometry type was specified as general. Rectangular type limits the geometry into only simple rectangular shapes. In contrast, general type allows users to create any type of geometry in addition to simple rectangular shapes.

4.4.2 Time information

The models were run for 6000 days to obtain stable initial pressure head distribution. For the subsequent simulations of ambient and flooded conditions, simulation time was set as 30. Models frequently crashed when lengthier simulations were attempted with weather data that includes precipitation and evaporation. Thus, the simulation time was shortened to 30 days to preserve a relatively small mesh and time step. As described in 4.7 (below), the upper boundary was specified as the atmospheric interface in the ambient condition. Time variable boundary conditions were added to include weather data needed to calculate atmospheric flux. Maximal and minimal time

steps were adjusted to be as small as possible such that the models do not collapse.

Table 4.2 Time information

Time units	Time discretization					Number of time variable boundary records
	Initial time	Final time	Initial time step	Minimum time step	Maximum time step	
Days	0	30	0.1	0.01	1	30

4.4.3 Water flow information

4.4.3.1 Soil hydraulic model

The Van Genuchten model (Equation 4.1) was selected for reference soil hydraulic parameters as it is widely used model and with parameterization given in the AMEC report.

$$\theta(h) = \begin{cases} \theta(h) = \theta + \frac{\theta_s - \theta_r}{\left[1+|\alpha h|^h\right]^m} & h < 0 \\ \theta_s & h \geq 0 \end{cases} \tag{4.1}$$

$$k(h) = K_s S_e^l \left[1 - \left(1 - S_e^{1/m}\right)^m\right]^2 \tag{4.2}$$

where

$$m = 1 - 1/n, \quad n > 1 \tag{4.3}$$

in which θr and θs denote the residual and saturated water content, respectively; Ks is the saturated hydraulic conductivity, α is the inverse of the air-entry value (or bubbling pressure), n is a pore-size distribution index, and l is a pore-connectivity parameter assumed to be 2.0 in the original study of Brooks and Corey (1964).

When the Van Genuchten model is used, users are required to select either non-hysteretic description or hysteretic description.

4.4.4 Hydraulic parameters

Table 4.3 shows hydraulic parameters for a selected cross section. Although there were more layers in the AMEC report, some layers were combined as they had very similar values. Soil water retention curves were generated based on the hydraulic parameters and shown in Figure 4.2. Material 1 and 6 have much higher hydraulic conductivity values than other materials. The material distribution is discussed later in 4.7.2.

Table 4.3 Hydraulic parameters

Material No.	Name	θr	θs	α, m^{-1}	n	Ks, m/day
1	SPSM	0.1563	0.3830	1.5328	8.3990	12.1006
2	CL	0.1745	0.4400	0.5610	2.2570	0.0006
3	C	0.1137	0.3330	0.4158	1.9978	0.1015
4	SM	0.0750	0.3790	0.6758	4.7358	0.1155
5	SP	0.0967	0.3830	0.3383	3.7607	0.1167
6	Toe Drain	0.0450	0.4300	4.4200	2.6800	7.1323

*Qr: residual water content
Qs: saturated water content
SPSM: poorly graded SAND with silt and gravel, CL: inorganic clay, C: clay, SM: silty sand, SP: poorly-graded sand, Toe drain: gravels filled in trenches

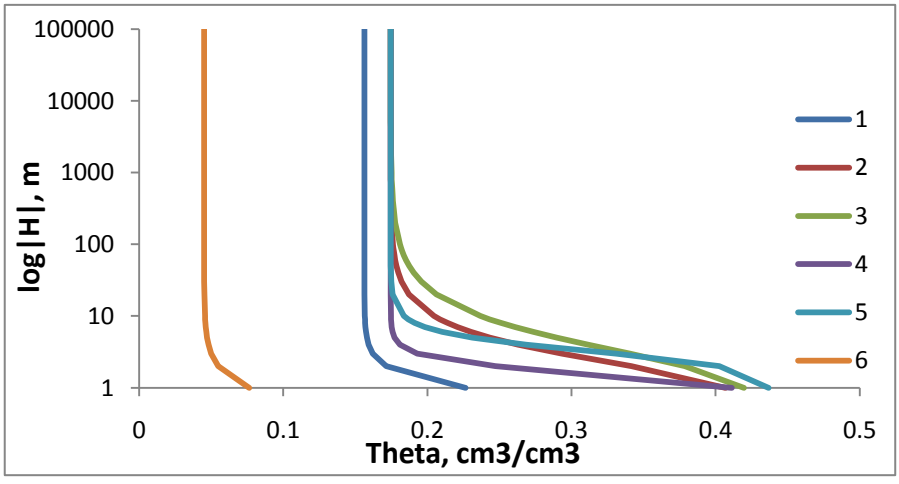

Figure 4.2 Soil water retention curves

4.5 Variable boundary conditions

Precipitation and evaporation data were assigned as time-variable boundary conditions. The data were obtained from New Mexico Climate Center (NMCC) website. The Albuquerque Bosque station (35.261389, 106.596111) was chosen as it would reasonably show climate conditions near the levees. The data were derived from the station for January 1, 2005 through December31, 2005. Data from 2005 was selected because the recorded precipitation was the greatest in the last 8 years. Since the total simulation period was 30 days, weather data for 30 days were selected from February 7, 2005 to March 3, 2005 when there was substantial precipitation.

HYDRUS-2D also requires evaporation data although NMCC data does not provide evaporation data. So, HYDRUS-1D was used to calculate evaporation from the NMCC meteorological data. To calculate evaporation in HYDRUS-1D, five types of data are needed in addition to precipitation (Figure 4.4): the maximum and minimum temperature, humidity, wind speed, and sunshine hours (Figure 4.3).

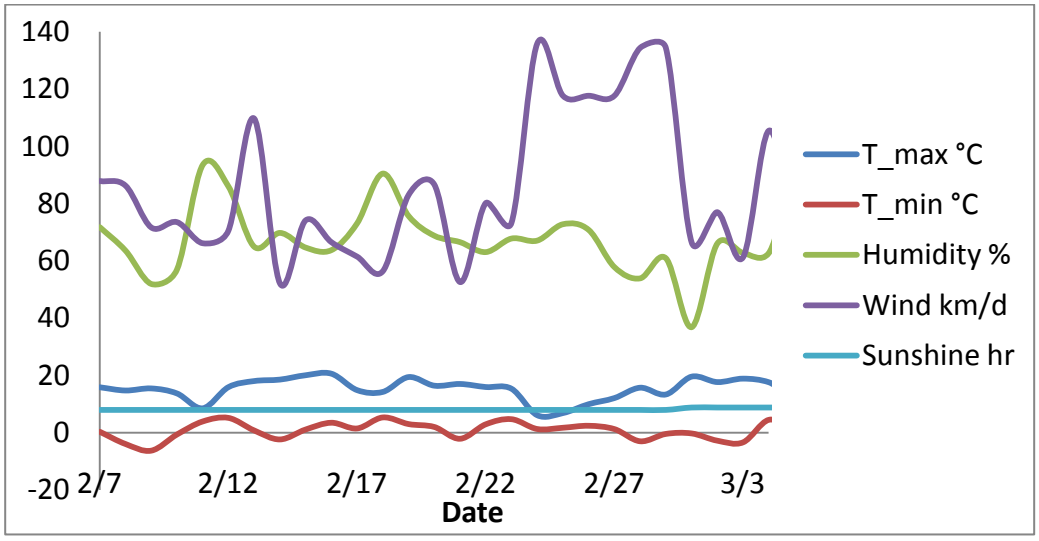

Figure 4.3 the maximum and minimum temperature, humidity, wind speed, and sunshine hours

Applying these five data sets and precipitation data in HYDRUS-1D, potential daily evaporation was calculated based on Penman-Monteith combination equation (Equation 4.4).

$$\lambda ET = \frac{\Delta(R_n - G) + \rho_a C_p \frac{(e_s - e_a)}{r_a}}{\Delta r \left(1 + \frac{r_s}{r_a}\right)} \tag{4.4}$$

where λ is the latent heat of vaporization of water (J kg-1), E is the rate of evaporation (kgm-2s-i), R_n is net radiation, G is the soil heat flux, (e_s - e_a) represents vapour pressure deficit, ρ_a is mean air density at constant pressure, c_p is the specific heat of the air, Δ represents the slope of the saturation vapor pressure temperature relationship, γ is the psychrometric coefficient, and r_s and r_a are the (bulk) surface and aerodynamic resistances (Allen et al, 2000).

Table 4.4 shows meteorological parameters used in HYDRUS-1D. The parameters and precipitation data (Figure 4.3) were used to calculate potential evaporation based on Penman-Monteith combination equation. Further details about calculating some values on Penman-Monteith combination equation can be found in FAO (1999).

Table 4.4 Meteorological data

Radiation type	
Potential Radiation	
Geographical and meteorological parameters	
Latitude, degree	Attitude, m
35	1500
Angstrom values (short wave radiation)	
Angstrom values a	Angstrom values b
0.25	0.5
Cloudiness effect on long wave radiation	
a1	a2
0.9	0.1
Emissivity effect on long wave radiation	
al	bl
Measurement heights	
Wind speed (cm)	Temperature (cm)
200	200
Cloudiness	
Sunshine	
Crop data	
No crop	Albedo
	0.3

*Relative humidity specified.
Further details can be found in HYDRUS-2D Manual (1999)

The Penman-Monteith equation uses only meteorological data, so potential evaporation is independent of other input data such as soil type. Figure 4.4 shows daily mean precipitation and potential daily evaporation derived from Albuquerque Bosque station data.

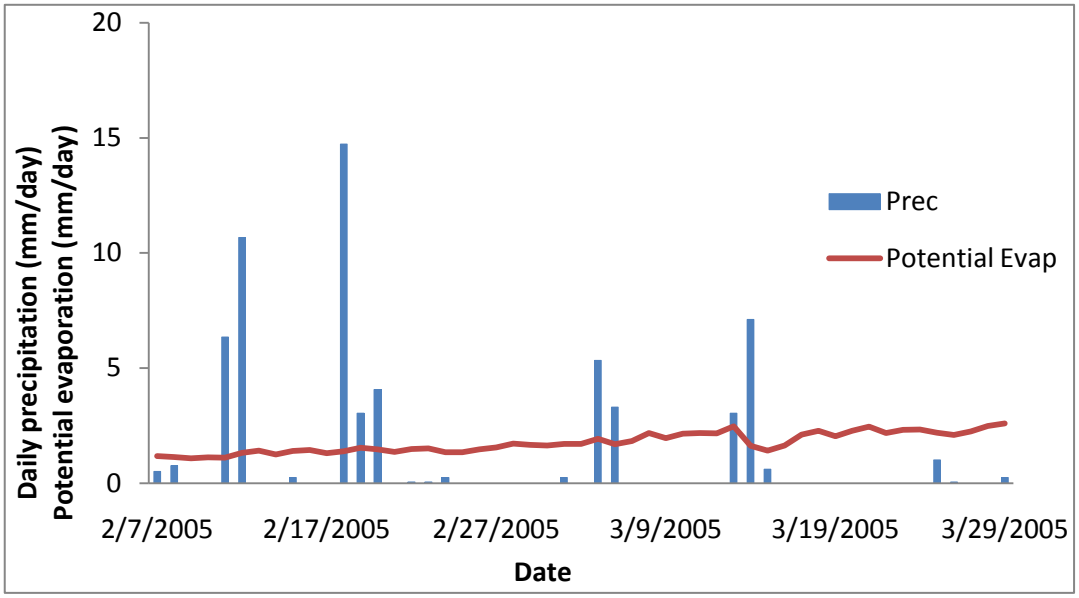

Figure 4.4 Daily precipitation and evaporation

4.6 Meshgen-2D

4.6.1 Geometry

Two types of geometry were prepared assuming different drainage system. Toe drain (Figure 4.5) is a typical design for levee drainage, and the levees along the MRG are usually constructed with this drainage system. In addition to the conventional toe drain that incorporates a perforated pipe in a gravel-filled tench, a geosynthetic edge drain was added to evaluate its function compared with a conventional toe drain (Figure 4.6). Geosynthetics are frequently used for pavement edge drain. A geocomposite edge drain may be a good alternative drain system for a levee. Typically, the geocomposite is made of a geonet sandwiched with two geotextiles. In a geocomposite edge drain, there is no need for a longitudinal trench; accordingly, installation and maintenance is easier than for the designs with drainage pipes. The basic geometry of the levee and the toe drain

were obtained from AMEC report.

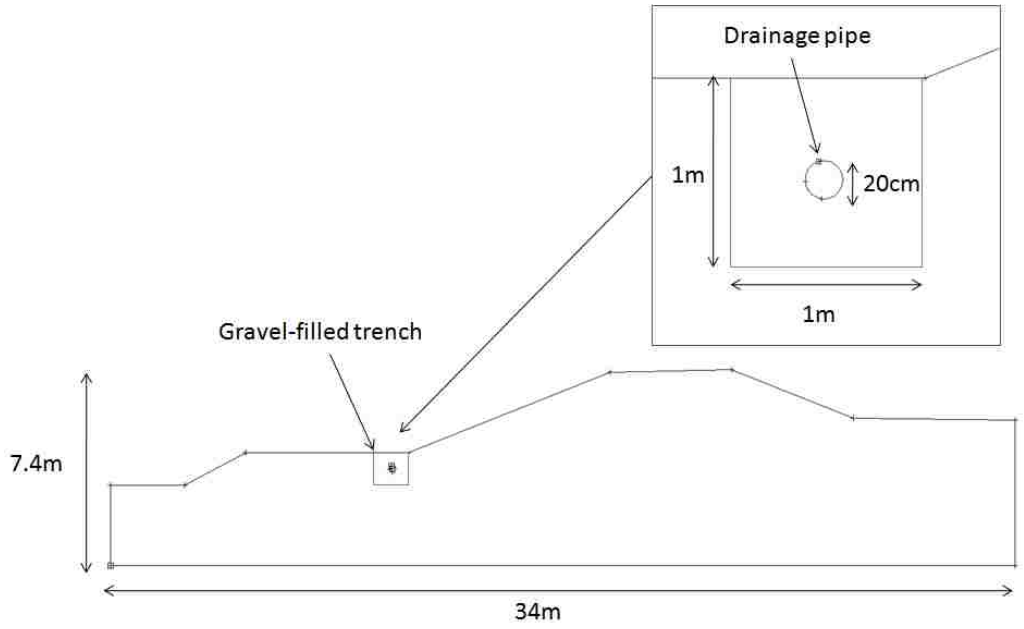

Figure 4.5 Toe drain

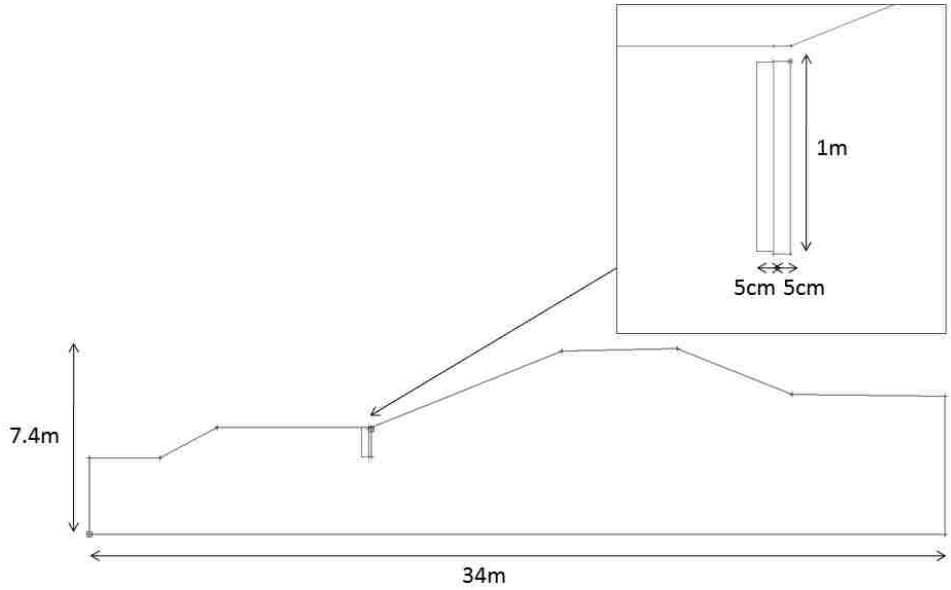

Figure 4.6 Geocomposite edge drain

4.6.2 Mesh creation

The mesh was created with 200 total nodes. The default value is 120 nodes, but it was increased to 200 to increase simulations accuracy, and to prevent model collapse during iterations. The mesh is denser in the upper portion and near the toe drain pipe as those parts are expected to have more changes in water movement than at the base.

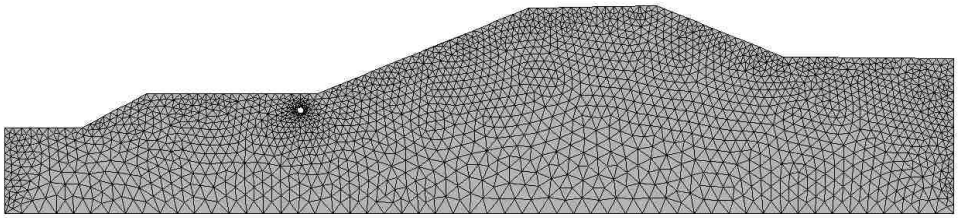

Figure 4.7 Mesh

4.7 Boundary module

4.7.1 Boundary conditions

For ambient simulations, atmospheric boundary conditions were applied at the soil surface (Figure 4.8).

For flood condition, flood water was introduced as constant pressure head boundary (Figure 4.9). Flood depth, associated with the 100-yr flood, was applied on the river side to measure the discharge rate into toe drain with each flood depth. For both the ambient and flood conditions, the bottom boundary was specified as no flux so that water movement into toe drain and ditch could be observed. The pipe was modeled as a seepage face as was the geocomposite edge drain.

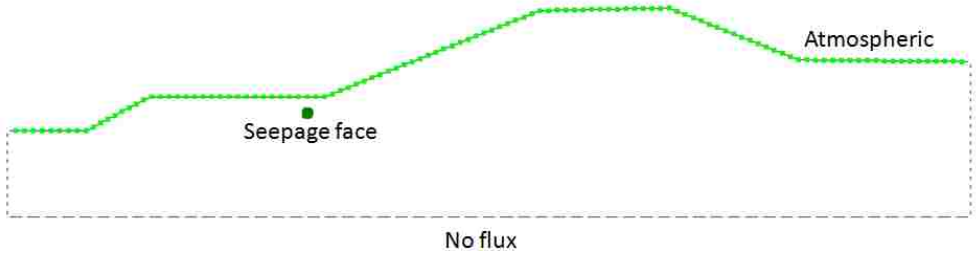

Figure 4.8 Boundary condition for ambient condition

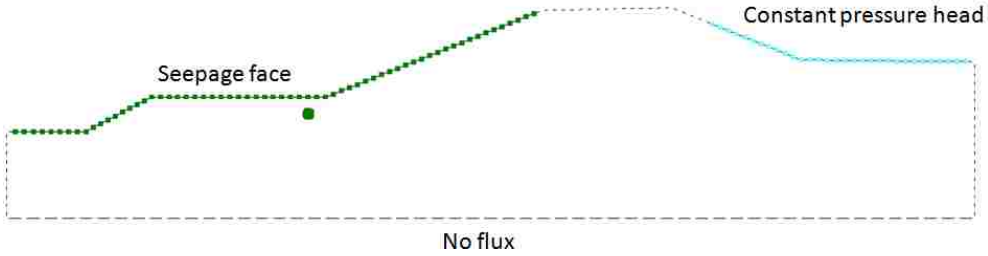

Figure 4.9 Boundary condition for flood conditions

4.7.2 Material distribution

Material distribution is shown in Figure 4.10. As mentioned, properties and distribution of materials were obtained from AMEC report, and hydraulic properties are shown in Table 4.2. Materials can be assigned in each node. The most permeable material, material number 1, is located beneath the levee structure.

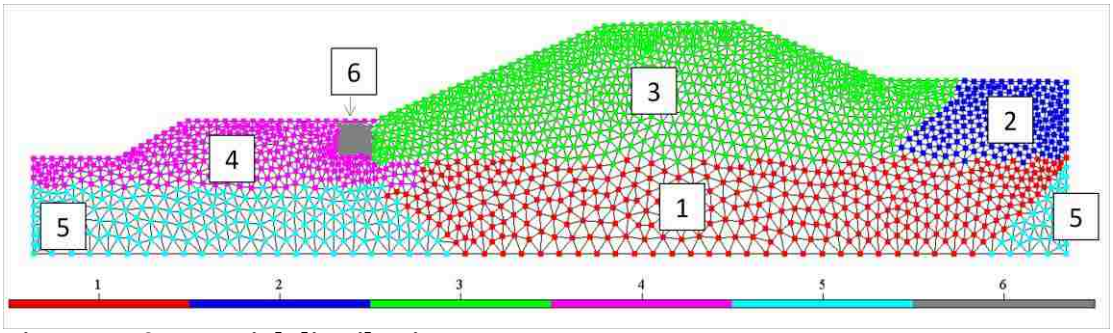

Figure 4.10 Material distribution
*The material numbers are corresponding to Table 4.2

4.7.3 Initial condition

Figure 4.11 shows the initial condition for both ambient and flood conditions. It was specified as pressure head distribution.

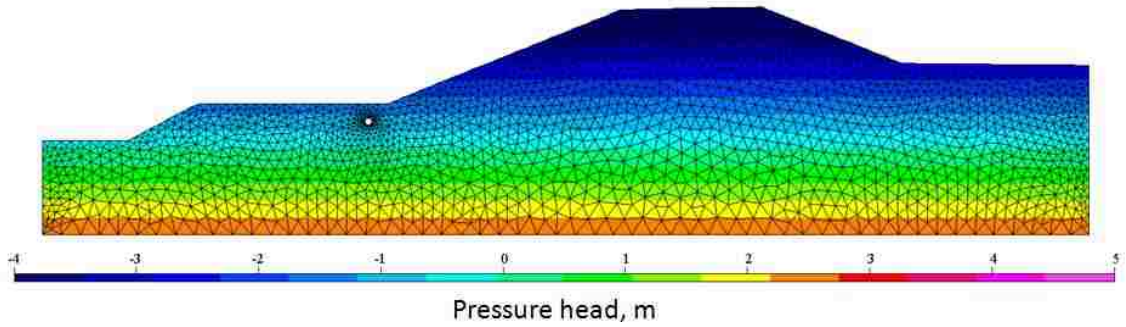

Figure 4.11 Initial condition

4.8 Results

4.8.1 Ambient condition

As expected, the soil near the drain did not saturate, and there was no drainage. The pressure heads were nearly identical for both drainage system as shown in Figures 4.12 and 4.13.

The water table remained close to the initial condition after weather events. Although precipitation and evaporation caused oscillation in groundwater levels of about 10 cm, it returned to original water table within several days. Pressure head responded to precipitation in the upper part of the levee even though pressure head in the drainage area remained unchanged.

High pressure head was observed in one part near the river side. This is probably a consequence of different moisture characteristic curves in material 2 and 1. In dry area like New Mexico, even very small differences in water content may result in differences in root growth and proliferation.

Water movement occurred mainly in the upper part and material 1. Other areas remained mostly inactive in ambient condition.

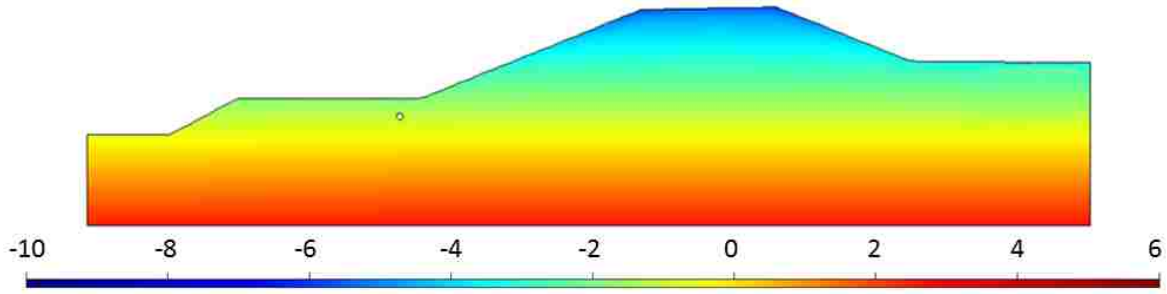

Figure 4.12 Pressure head distribution, ambient condition, toe drain, unit: m, day=30

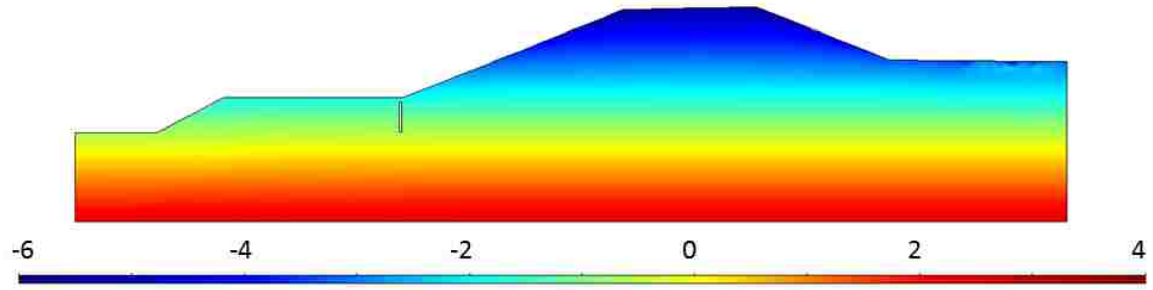

Figure 4.13 Pressure head distribution, ambient condition, edge drain, unit: m, day=30

4.8.2 Flood condition

Figure 4.14 shows the result of the flood simulation with a toe drain geometry. Flood water raised groundwater levels in both the river side to the ditch side.

After the bottom half of the toe drainage area (material 6) got saturated, water was immediately drained through the drain pipe, and the top half remained dry. In this simulation, the toe drainpipe was described as circular seepage face. As a result, more than 95% of water moved into pipe from the bottom of the pipe (Figure 4.15). Although the ditch and some parts of the levee structure are also specified as seepage face, as

shown in Figure 4.16, most water is drained through toe drain, in particular, through the bottom half.

It was shown that the bottom half of the drainage area had higher moisture content, which may encourage roots to proliferate.

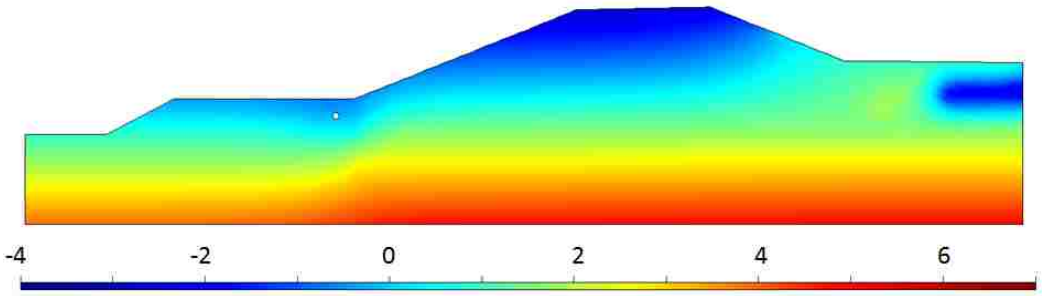

Figure 4.14 Pressure head distribution, flood condition, toe drain, unit: m, day=30

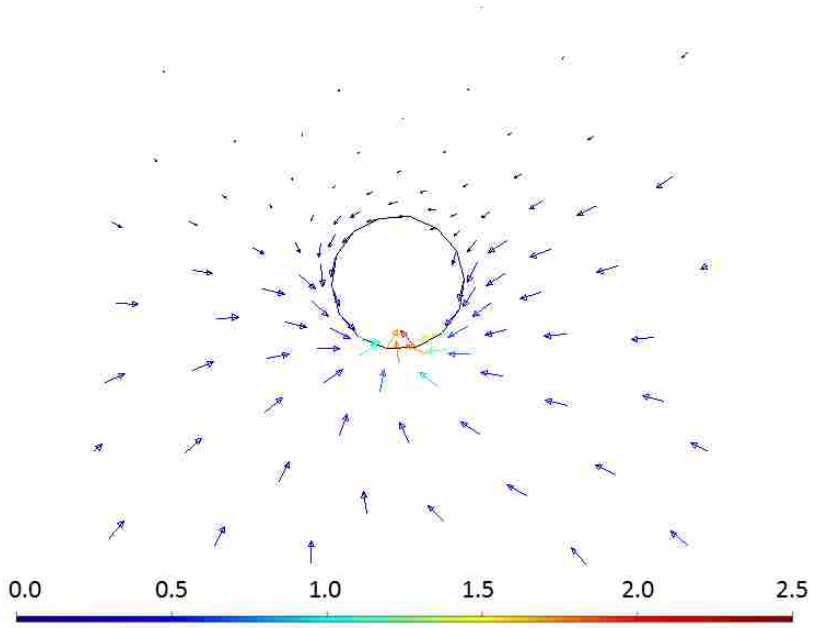

Figure 4.15 Water flow velocity near toe drain, day=30, m/day

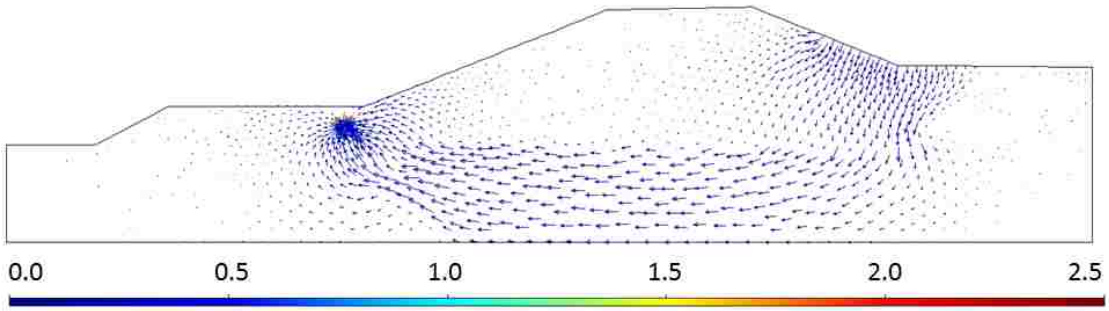

Figure 4.16 Water flow velocity (arrows), toe drain, day=30

Figure 4.17 shows the result of the simulation with the geocomposite edge drain when the riverside is flooded. With the geocomposite edge drain, the drainage area did not have as great of moisture content as did the model with the conventional toe drain. The drainage area refers to the area on the right side of the edge drain which is filled with coarse drainage materials (gravels). The bottom of the drainage area has water content of approximately 0.35, while water content of the same area was about 0.4 in the levee with the toe drain system. As shown in Figure 4.18, water is drained through the entire seepage face.

Figure 4.19 describes water flow direction through the levee. Similarly to the toe drain simulation, flood water flowed under the levee structure, and is drained through the geocomposite edge drain. Only a small amount of water reaches the ditch.

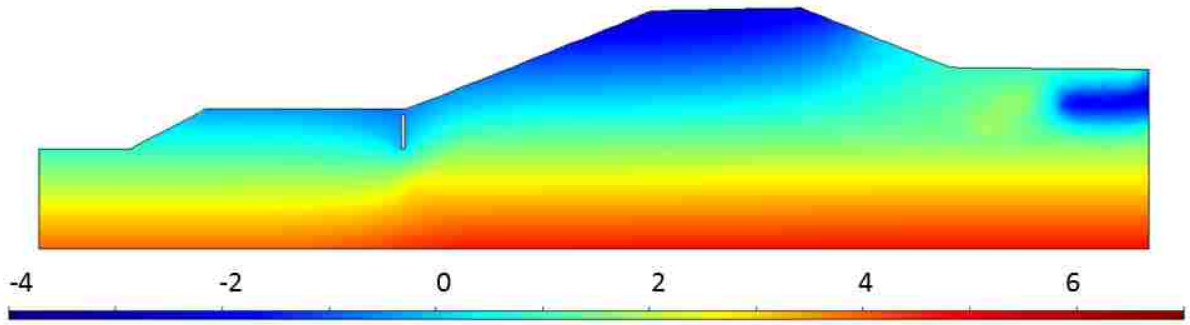

Figure 4.17 Water content distribution, flood condition, edge drain, unit: m, day=30

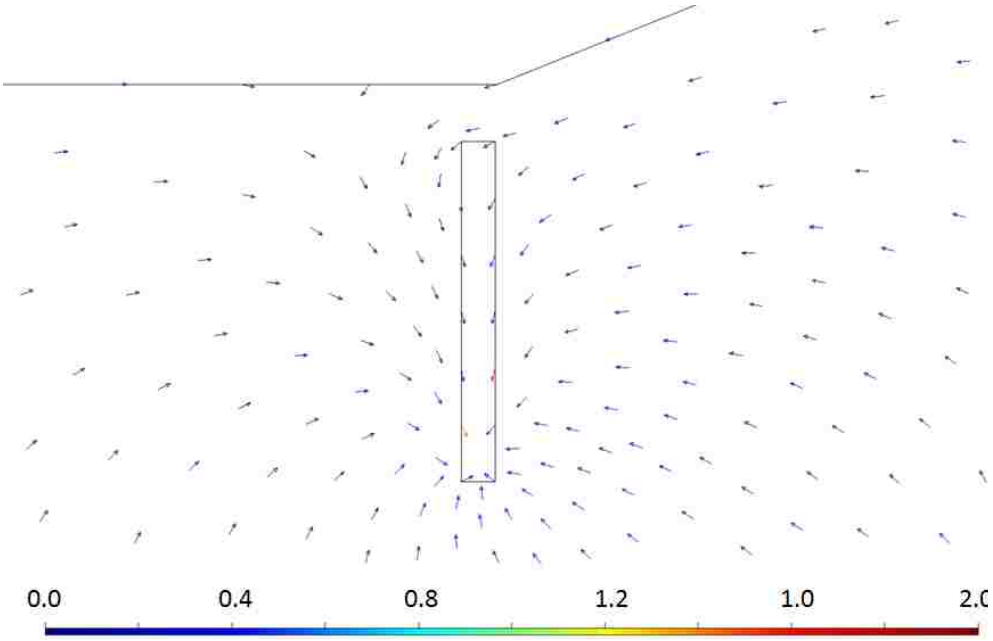

Figure 4.18 Water flow velocity near edge drain, day=30, m/day

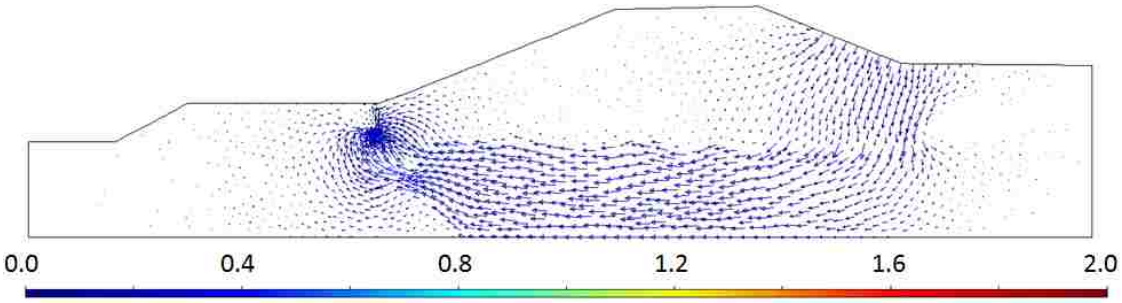

Figure 4.19 Water flow velocity (arrows), edge drain, day=30, m/day

Figure 4.20 shows the cumulative discharge from the seepage faces in response to the flood event. In the levee with a toe drain, discharge through the seepage face increased after day 5, upon saturation of the drainage material (gravels) adjacent to the edge drain. As the drainpipe was placed in the center of the drain material, drainpipe did not function until water accumulated in the material around the drainpipe. The drainpipe was described as the seepage face in the model so that it allowed water to be drained at any point along the drainpipe. However, perforated pipes used in drainage systems will have different shapes. For example, some pipes may have infiltration area only on the upper part of them. If this is the case, the bottom half should be specified as no flux boundary, not the seepage face. It will take more time to drain excess water than in the current model.

In these simulations, the geocomposite edge drain could remove excess water from the levee slightly faster than the conventional toe drain (Figure 4.20).

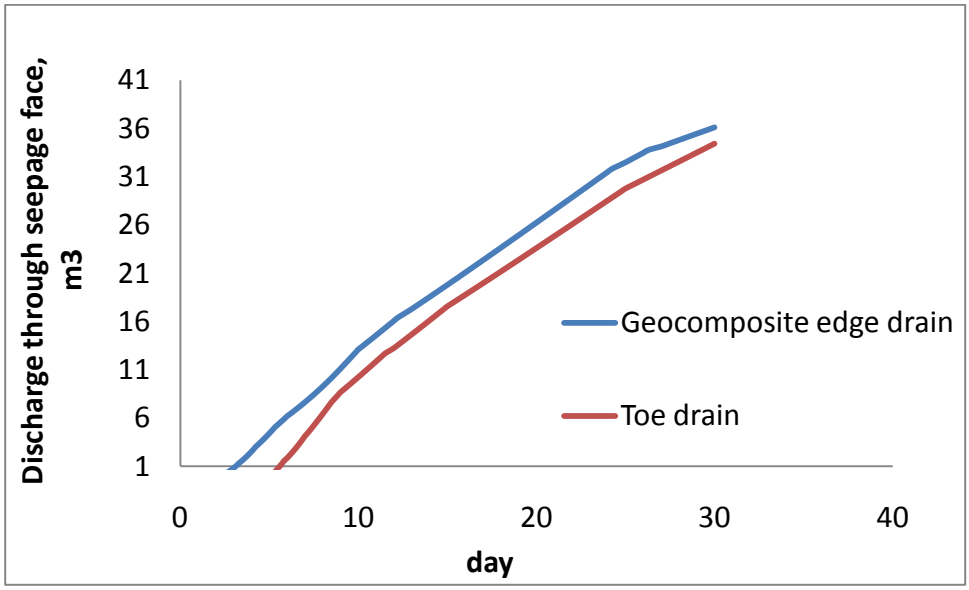

Figure 4.20 Cumulative discharge through the seepage faces

4.9 Conclusion

4.9.1 Summary of the results

Ambient condition

Weather events such as precipitation and evaporation did not affect drain function as the levee was not saturated. Most precipitation infiltrated into only upper part of the levee structure, and groundwater levels barely changed with weather events. Since the drainage areas remained relatively dry, the results did not explain the observation that roots tend to grow into drainpipes.

Flood condition

The flood simulation significantly raised the water table. Relatively high moisture content was observed in the drainage area with the toe drain; in contrast, the geocomposite edge drain remained less wet during the simulation period. The drainage area had moisture content of 0.35 in the geocomposite edge drain, while moisture content in the same area was 0.4 in the toe drain. More than 95 % of water was drained through the toe drain or the edge drain, rather than through the ditch. The geocomposite edge drain removed remove excess water better than the conventional edge drain.

4.9.2 Discussion

4.9.2.1 Limitations of the models

One of the main purposes of this research was to estimate the moisture condition in the vicinity of levee drains so as to provide some insight into why roots tend to grow into drainpipes at levees. It was shown that the toe drain had the possibility to proliferate root growth when the riverside is flooded; however, an event with a flood depth of 1m has not occurred in Albuquerque during the last 50 years. The flood depth is associated with a 100-yr flood. The 100-yr flood with a peak discharge of 19200 cfs has not been observed in Albuquerque since 1946. Under ambient conditions, the drainage areas remained relatively dry, and the model results did not reveal reasons for root intrusion into drain pipes.

In the bench-top experiments described in the chapter 3, fine soil was found accumulating in the bottom of the drainage area. This soil was likely washed down from the upper parts of the columns. Also, the gravel filter itself might have contained significant fine soil. Fine soil retains moisture, and this may eventually induce fine root

proliferation. If fine soil built up in the drainage area or inside of the drain pipe in the levee, it may be why roots proliferate into the drain pipe without flood events. This suggests the importance of filters.

4.9.2.2 Recommendations for further research

The initial condition used for the simulations contained extremely dry soils in the upper part of the levee structure. However, during certain times, the levee may have more moisture from precipitation events and groundwater table change. Therefore, additional simulations with different initial conditions may yield different results. A simulation for drought and expected climate scenarios should be considered. An effect of flood duration on the results should also be considered.

CHAPTER 5: CONCLUSION

5.1 Estimating tree root encroachment on levees

Tree encroachment on levees may decrease levee stabilities by clogging levee drainage systems. To prevent root intrusions into levee drainage systems, it is necessary to have a proper understanding of root growth in the riparian forest. High-resolution aerial photography was utilized to estimate tree crown size. The results were verified with field observations. Although this method was capable of measuring large tree canopies in a simple vegetation community, it was unable to accurately measure tree crowns in a complex vegetation community containing various types of shrub species.

Furthermore, the horizontal extent of tree root distributions was estimated using tree crown sizes using an assumed relationship between the crown size and horizontal root extent. It appeared that some cottonwood roots could reach the levee, and possibly threaten drainage systems.

GIS-based measurements have the potential to be used to estimate root encroachment on levees, in particular, for sites with simple vegetation communities. Although field observations can be perform in limited areas due to their laborious work, field observation remains the preferred method to estimate tree root encroachment on levees.

5.2 Bench-top experiment of root barriers

If trees were observed near levees, drainage systems would need to be designed with special treatments that may prevent tree roots from clogging drainpipes. Geosynthetics are frequently used for filtration and separation in drainage systems. Bench-top experiments were conducted to assess the capability of geosynthetics to prevent root intrusions. Cottonwoods and willows were grown under several drainage

systems for 5 month. The results indicated that neither geotextile nor the geocomposite were capable of protecting drainage areas from the root encroachments. Also, root growth did not appear to vary with different drainage systems, sand and gravel.

If trees were observed near a levee on GIS-based measurements (Chapter 2), the best treatment would be tree removal as the experiments showed that geosynthetics are not capable of limiting root intrusion. Biobarrier, which is an herbicide-based geotextile, may be used as an alternative barrier although Biobarrier is more expensive than s simple geotextile.

Further experiments would be needed to suggest alternatives for vegetation management on levees.

5. 3 Numerical modeling

To design drainage systems that would not induce root proliferation, it is usuful to understand soil water movement within levees.

Numerical modeling using Hydrus-2D was conducted to calculate soil moisture conditions in a levee and its drainage systems. Higher moisture content in unsaturated soil is assumed to result in fine root proliferation, while root length extension is assumed to be carried out in drier soils. Conventional toe and the geocomposite edge drains were simulated. The models were run under ambient and flooded conditions.

The results showed that functioning in both drainage designs was close to identical under the ambient conditions and it did not result in drainage. The conventional toe drain resulted in an area with higher moisture content under the flood condition. In contrast, the conventional toe drain removed excess water slightly faster.

The geocomposite edge drain would be recommended because drain function of the geocomposite edge drain was slightly better than of the conventional toe drain.

Installation and maintenance of the geocomposite edge drain is less difficult. It is less expensive as there is no need for a drainpipe, and a gravel-filled trench may be smaller than the conventional toe drain.

Appendix-A: Root barrier information

1. Geotextile

Geotextile is water permeable geosynthetic comprised solely of textiles. There is also herbicide-based geotextile barrier which includes attached herbicide pellets. The herbicide geotextile is expensive, and did not show a significant benefit on the previous study. Geotextile is cost-effective material, that is easy to transport and install due to its light weight. However, simple geotextile is inferior in durability to geobarriers. Also, its puncture strength and sunlight durability is lower than those of a continuous barrier

2. Geocomposite

Geocomposites consist of various combinations of geotextiles, geogrids, geonets, geomembrane, and/or other materials (Koerner, 1994). They are typically used for separation, filtration, and/or drainage. As they are made of combination of several materials, they are much stronger and have longer longevity.

3. Product information –Typar, geotextile

Root barrier name: Typar

Manufacturer contact information:

Fiberweb plc (http://www.fiberweb.com)

70 Old Hickory Blvd. Old Hickory, TN 37138

Phone: (800)284-2780

E-mail address: rbergh@fiberweb.com

Material: nonwoven polypropylene geotextile fabric, water permeable

Figure A-1 Geotextile

4. Product information –Geocomposie–

Root barrier name: 2sided Geocomposite

Manufacture contact information:

AGRU AMERICA, INC.

500 Garrison Road, Georgetown, South Carolina 29440 USA

Phone: (843)546-0600

Email address: salesmkg@agruamerica.com

Material: The geotextile is bonded to the geonet with a hot knife application allowing for high bond strength without the reduction of transmissivity values of other processes

Figure A-2 Geocomposite

Appendix-B: Grain design of gravel filters

1. Objective

Grain size analysis was conducted in order to design appropriate drainage gravel for the bench-top experiment

2. Design Reference

NRCS-Part 633 National Engineering Handbook, Chapter 26 Gradation Design of Sand and Gravel Filters

3. Symbols used

D refers to filter, d refers to base soil

4. Procedure

i. Plot the gradation curve (grain-size distribution) of the base soil material.

Table B-1 The gradation curve

Sieve Size	% Passing
No.10	100
No.16	92
No.40	38
No.50	28
No.100	15
No.200	12

ii. skip since % retained on #4 sieve=0

iii. Base soil category #4, Sands and gravel, i.e. % passing #200 sieves=5%≤15%

iv. Maximum allowable $D_{15} \leq 4 \times d_{85}$ of base soil after regarding, $D_{15max} \leq 4 \times d_{85} = 4 \times 1.09mm = 4.36mm$ (Control point 1)

v. Minimum allowable $D_{15min} \geq 4 \times d_{15} = 4 \times 0.149mm = 0.596mm$

$4.36mm \geq D_{15} \geq 0.596mm$

Ratio of max and min D_{15} sizes must be ≤5

$D_{15max}/D_{15min} = 4.36mm/0.596mm = 7.32$

Since gravel has to work as a filter, D_{15min} is unchanged.

Adjusted D_{15max}=0.596 x 5=2.98mm (Control point 2)

vi. Adjust limits of design filter band so that coarse and fine sides have a coefficient of uniformity of and fine sides have a coefficient of uniformity of 6 or less. Calculate D_{10max}, D_{60max}, and D_{10min}

$D_{10max}=D_{15max}/1.2=2.98/1.2=2.48$mm

D_{60max}=6 x D_{10max}=6 x 2.48=14.88mm (Control point 3)

$D_{60min}=D_{60max}/5=14.88/5=2.979$mm (Control point 4)

vii. Determine D_{5min} and D_{100max}

Determine the maximum D90

$D_{10min}=D_{15min}/1.2=0.596/1.2=0.5$mm

D_{90max}=25mm (Control point 7)

viii. Connect control points 4, 2, and 5 to form a partial design for the fine side of the filter band. Connect control points 6, 7, 3, and 1 to form a design foe the coarse side of the filter band.

5. Results

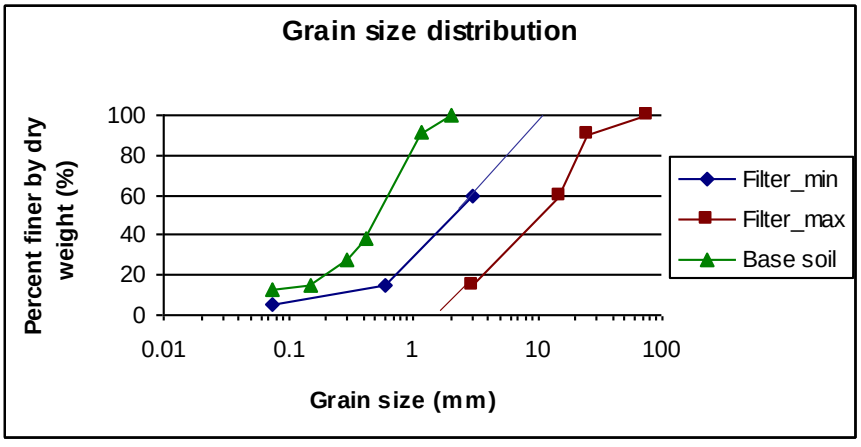

Figure B-1 Grain size distribution

*Grain size distribution of gravel filter should be between "Filter min" and "Filter max"

Appendix-C HEC-RAS project

1. Introduction

The main purpose of this project was to determine flood depth in the riparian corridor in order to apply the results for the numerical simulations.

Method

1.1 HEC-RAS input data

1.1.1 Geometric data

Cross section data was created based on TIN data by Kelly Isaacson. The reach begins at the north of Alameda bridge (35°12'46.80"N, 106°37'1.20"W), and ends near the Central bridge (35° 4'55.20"N, 106°40'22.80"W) (Figure.1). For the mail channel, either 0.025 or 0.05 was applied as Manning's n values. These values are used in the current Corp of Engineering MRG HEC-RAS model. In their model, n=0.08 is used for the floodplain; however, in this study, three other values listed in Table.1 were applied to evaluate the effect of n values on flood depth. The floodplains in all cross sections of the reach were set to have identical n value in order

to describe uniform vegetation type throughout the reach.

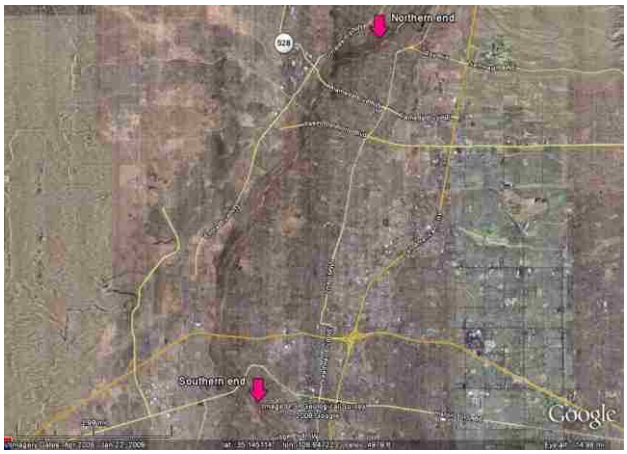

Figure D-1 Study area

Table D-1 Manning's n values (Chow, 1959)

	Willow	Tree	Grass
n	0.15	0.1	0.03

1.1.2 Steady Flow data

Seven flow rates were applied as steady flow data (Table.2). These flow rates data was obtained from Middle Rio Grande Frequency Study Report by US Army Corps of Engineers. Flow rates were applied at the northern cross section of the reach. Critical depth or normal depth was applied as flow boundary to understand how the choice of boundary condition affects results.

Table D-2 Flow rates

Exceedance probability		Peak flow
Percent	Year	cfs
50	2	6890
20	5	8220
10	10	10500
2	50	16300
1	100	19200
0.5	200	22100
0.2	500	16700

1.2 Data analysis

1.2.1 Cross section

Figure.2 shows two cross sections selected for data analyses: the alameda cross section in the south of Alameda bridge (35° 11'27.6"N, 106° 38'49.2"W), and the central cross section near the north of Central bridge (35° 5'27.6"N, 106° 41'6"W). As seen in the picture, the dominant species in each site is trees, in particular, Cottonwood. Although n=0.10 for trees seems to be appropriate, other two n values were applied so that how flood depth will be changed if the riparian corridor is

covered by other types of vegetation.

Figure D- 2 Cross sections

1.2.2 Flood depth

Flood depth was defined as a height of water surface from the levee base (Figure.3). Flood depth was calculated for each flood event. As flood depth at both right and left

side of the main channel was very similar, it was measured at only right side.

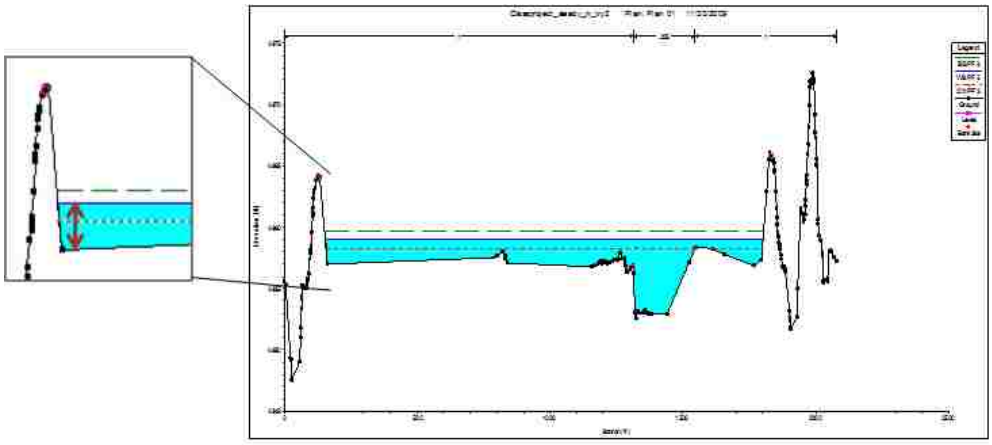

Figure D-3 Flood depth measurement

2. Results

2.1 Critical depth as boundary flow

2.1.1 Central Bridge

Figure.4 and Table.3 show flood depth caused by each flow rates at the central cross section. Flood depth is nearly identical in each n value if the flow rate is low. As flow rates increase, the difference of food depth between each vegetation type increases. Willow and trees give similar curve while grass cover significantly lowers flood depth. 4720 cfs was obtained as the minimum flow rate to achieve flood condition. Flooding does not occur if the flow rate is lower than 4720 cfs. Hydrograph was obtained from USGS stream gage no. 08330000 at Central Bridge (Figure.5). After the biggest recorded flood event in 1942, peak discharge has been decreasing. As peak discharge exceeds 4720 cfs occasionally, the levees are considered to meet flood conditions every several years. Flood depth does not exceed 2 ft since 1943 if the

riparian corridor is covered thoroughly with tree. If it is covered with grass, instead of trees, the maximum flood depth would decrease to approximately 1 ft.

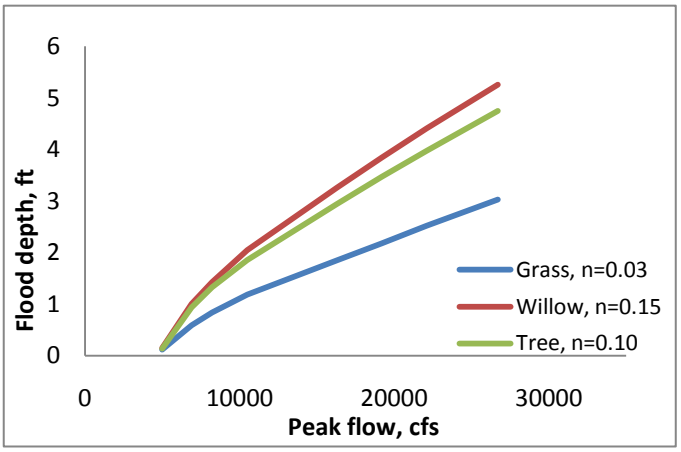

Figure D-4 Flood depth at the central cross

Table D-3 Flood depth

Peak flow	Exceedance probability	Flood depth, ft		
		Grass	Willow	Tree
cfs	year	n=0.03	n=0.15	n=0.10
6890	2	0.59	1.01	0.94
8220	5	0.84	1.43	1.33
10500	10	1.19	2.05	1.86
16300	50	1.85	3.26	2.94
19200	100	2.18	3.84	3.47
22100	200	2.52	4.41	3.97
26700	500	3.03	5.26	4.75

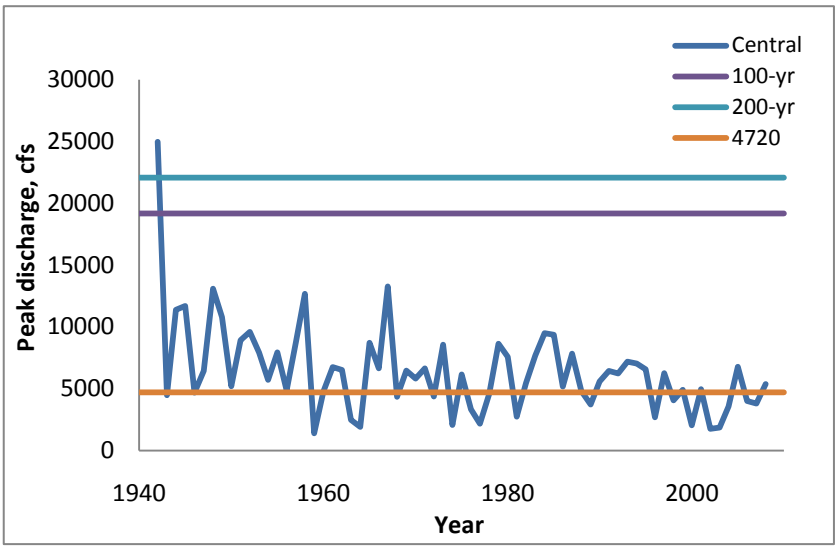

Figure D-5 Peak discharge hydrograph

2.1.2 Alameda Bridge

Although the trends of plots are similar to those of the central bridge cross section, flood depth is lower as it has deeper main channel at the alameda cross section (Figure.6 and Table 4). At the alameda bridge cross section, flood occurs when flow rate is higher than 10000 cfs while central cross section meets flood condition with 4720 cfs. The alameda bridge cross section is located between Alameda Bridge and Paseo del Norte Bridge. As they have gages in each point, two hydrographs were

obtained (Figure.7). They show that the flow rates did not exceed 10000 cfs last 20 years. Therefore, the alameda bridge cross section did not meet any flood conditions last 20 years.

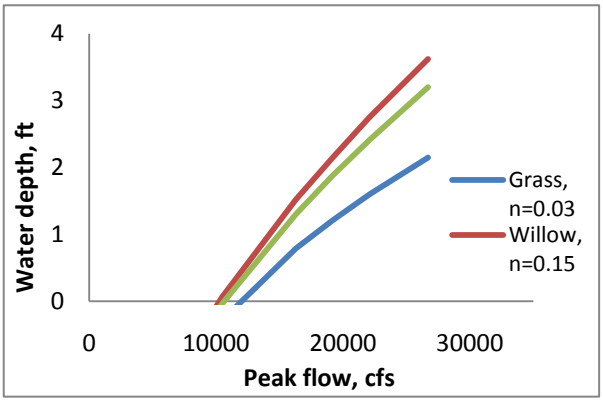

Figure D-6 Flood depth at the alameda cross

Table D-4 Flood depth

Peak flow	Exceedance probability	Flood depth, ft		
		Grass	Willow	Tree
cfs	year	n=0.03	n=0.15	n=0.10
6890	2	0.00	0.00	0.00
8220	5	0.00	0.00	0.00
10500	10	0.00	0.07	0.00
16300	50	0.79	1.52	1.30
19200	100	1.21	2.15	1.88
22100	200	1.60	2.75	2.41
26700	500	2.15	3.62	3.20

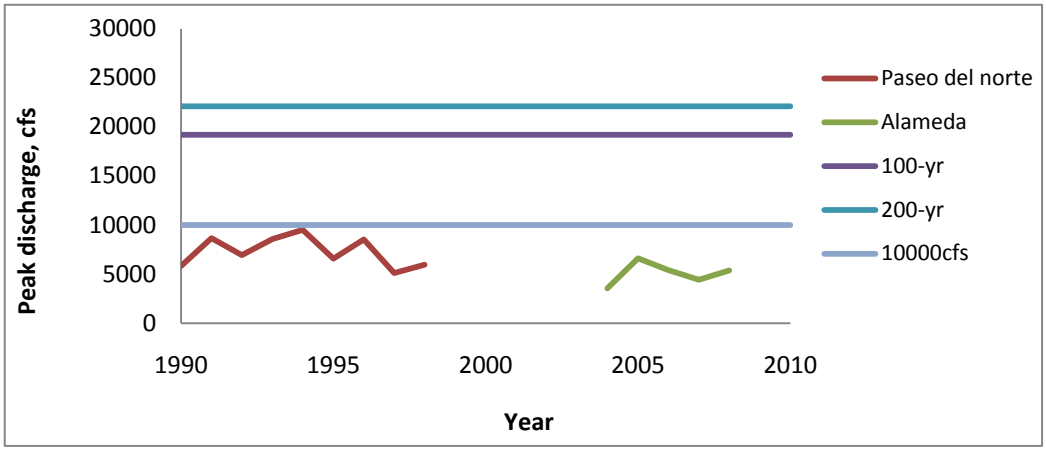

Figure D-7 Peak discharge hydrograph

2.2 Normal depth as boundary flow

Critical depth was applied as boundary condition in the first simulation. The result was used to calculate energy slope for the reach (average energy slope=0.000902). Normal depth was used as boundary flow in the next simulation. This boundary condition requires the input of average energy slope. 0.000902 was used for the slope, and the results were compared with the first simulation. Flood depth was approximately identical in two simulations. In this study, the different boundary flow did not have influence on flood depth.

2.3 Conclusion

It was proven that Manning's n value has strong influence on flood depth in the riparian corridor. The riparian corridor along the middle Rio Grande is, in general, covered with trees with understory species; however, if it is covered with other types of vegetation, the flood depth can be nearly 0.5 ft higher or 2 ft lower depending on the vegetation type. Decrease of peak flow rates in recent years strongly affects flood

depth, and the levees did not meet flood condition higher than 2ft last 50 years. The difference of flood depth caused by n values becomes significant when flow rates are higher. In this study, only two cross sections were used in data analyses. As each cross section has unique geometry, different answer could be obtained if other cross sections were selected. Geometric data has 262 cross sections in total. Analyzing every cross section manually is time-consuming process, which also requires engineering judges. In order to analyze flood depth throughout the reach, new method must be developed to ease the process. Moreover, the cross section data includes unrealistic irregularity in floodplains. Although TIN data is largely accepted as an efficient method in generating cross sections for large areas, more precise method should be developed for this type of study.

List of References

Abernethy, B., and I.D. Rutherfurd, 2000, The effect of riparian tree roots on the mass-stability of riverbanks. Earth Surface Processes and Landforms 25: 921–937

Allen R., Pereira L., Raes D. and Smith M., 2000, FAO Irrigation and Drainage Paper No. 56 – Crop Evapotranspiration – Guidelines for Computing Crop Water Requirements FAO – , Food and Agriculture Organization reprort

American Society of Civil Engineers, 1998, River width adjustment I: Processes and mechanisms, Journal of Hydraulic Engineering 124:881–902

Brooks, R. H., and A. T. Corey, 1966, Properties of porous media affecting fluid flow, Journal of Irrigation and Drainage, 72(IR2): 61-88

Carlos Costa, Lianne M. Dwyer, Robert I. Hamilton, Chantal Hamel, Line Nantais and Donald L. Smith, A sampling method for measurement of large root systems with scanner-based image analysis, Agronomy Journal 92(4): 2000

Costello, L.R., C.L. Elmore, and S. Steinmaus. 1997. Tree root response to circling root barriers. Journal of Arboriculture 23(6): 211-–218.

Dengsheng, 2006, The potential and challenge of remote sensing-based biomass estimation, International Journal of Remote Sensing 27(7): 1297–1328

Dianne Elaine McDonnell, 2006, Scaling Riparian Evapotranspiration to Canopies along the Middle Rio Grande Corridor in Central New Mexico, Dissertation, University of New Mexico Department of Biology, Chapter 2. Classifying Canopy Vegetation along the Middle Rio Grande Riparian Landscape Hickin, E.J, 1984, Vegetation and river channel dynamics, Canadian Geographic, 28: 111–126

Food and Agriculture Organization of the United Nations, Expert consultation on revision of FAO methodologies for crop water requirements, *ANNEX V*, FAO Penman-Monteith Formula, Rome Italy, 1990.

Heede, B.H., and J.N. Rinne, 1990, Hydrodynamic and fluvial morphological processes and implication for fisheries management and research, North American Journal of *Fisheries* Management, 10: 249–268

Jeremy L. Weiss, David S. Gutzler, Julia E. Allred Coonrod, Clifford N. Dahm, 2003, Long-term vegetation monitoring with NDVI in a diverse semi-arid setting,central New Mexico, USA, Journal of Arid Environments 58: 248–271

Jim McKean, and Ken Inouye, 2001, Field evaluation of the long-term performance of geocomposite sheet drains, Geotextiles and Geomembranes 19(4): 213-234

Kremer, R.G., Running, S.W., 1993, Community type differentiation using NOAA/AVHRR data within a sagebrush-steppe ecosystem, Remote Sensing of Environment 46: 311–318

Mosley, M.P., 1981, Semi-determinate hydraulic geometry of river channels, South Island, New Zealand, Earth Surface Processes Landforms 6: 127–137.

Murgatroyd, A.L., and J.L. Ternan, 1983, The impact of afforestation on stream bank erosion and channel form, Earth Surface Processes Landforms, 8: 357–370

Murty, AVSR., Mathur, S. and Chandra, D. and Rao, K. N., 1994, Selection of Geotextile Filters Wrapped Around Pipes In Pavement Edge Drains, Geotextiles and Geomembranes, 13: 519—529

M. van Noordwijk, G. Brouwer, F. Meijboom, M. do Rosario G. Oliveira and A.G. Bengough, 2000, Trench profile technique and core break method, Root Method Chapter 7: 212-231

Newman, E. I., 1966, A method of estimating the total length of root in a sample. Journal of Applied Ecology, 3: 139-145

Nunnally, N.R., F.D. Shields, Jr., and J. Hynson, 1987, Environmental Considerations for Levees and Floodwalls, Environmental Management 11(2): 183-191

Patrick J. Marer, 1996, Sewer line root control, The manual published by the California Department of Pesticide Regulation

Shields, F.D., Jr., and D.H. Gray, 1992, Effects of woody vegetation on sandy levee integrity, Water Resources Bulletin, 28: 917–931

Simunek, J., M. Sejna, and, M. Th. Van Genuchten, 1999, HYDRUS-2D/MESHGEN-2D code for simulating water flow and solute transport in two-dimensional variably saturated media, IGWMC - TPS 53C, Ver. 2.01, International Ground Water Modeling Center, COlorado School of Mines, CO 80401

Sorin C. Popescu, Randolph H. Wynne, and Ross F. Nelson, 2003, Measuring individual tree crown diameter with lidar and assessing its influence on estimating forest volume and biomass, Canadian Journal *of* Remote Sensing, 29(5): 564–577

Stephen B. Allen, John P. Dwyer, Douglas C. Wallace, and Elizabeth A. Cook, 2003, Missouri river flood of 1993: Role of woody corridor width in levee protection, Journal of the American Water Resources Association , 39(4): 923-933

Stokes A., Fourcaud T., Hruska J., Cermak J., Nadyezdhina N., Nadyezhdin V., Praus L., 2002, An evaluation of different methods to investigate root system architecture of urban trees in situ : I. Ground-penetrating radar, Journal of arboriculture 28(1): 2-10

Thorne,C., I.Amarasinghe, J.Gardiner,C. Perala-Gardiner,R. Sellin M. Greaves, and J. Newman, 1997, Bank protection using vegetation with special reference to willows, Project record, Engineering and Physical Sciences Research Council Agency, Swindon, UK.

U.S. Army Corps of Engineers, 1978, Design and Construction of Levees, Engineer Manual 110-2-1913, Washington, D.C.

U.S. Army Corps of Engineers, 2008, Albuquerque west levee project environmental assessment, the final project report for the Albuquerque west levee project

U.S. Army Corps of Engineers, 2009, Engineering and Design: Guidelines for Landscape Planting and Vegetation Management at Levees, Floodwalls, Embankment Dams, and Appurtenant Structures, ETL 1110-2-571

U.S. Forest Service Rocky Mountain Research Station, 2008, Middle Rio Grande basin research report, a progress report from the middle Rio Grande ecosystem management research unit

Willy Dierickx, 1993, Research and developments in selecting subsurface drainage materials, Irrigation and Drainage System 6L 291-310

Wilson, A. D. and Lester, D. G., 2002, Trench inserts as long-term barriers to root transmission for control of oak wilt, Plant Disease, 86: 1067—1074

W. W. Wilhelm, J. M. Norman and R. L. Newell, 1983, Semiautomated X-Y-Plotter-Based Method for Measuring Root Lenghts, Agronomy Journal, 75:149-152